NASA TECHNICAL NOTE

NASA TN D-3933

NASA TN D-3933

THE STRUCTURE OF AN ATMOSPHERE FROM ON-BOARD MEASUREMENTS OF PRESSURE, TEMPERATURE, AND ACCELERATION

by Simon C. Sommer, Alfred G. Boissevain, Layton Yee, and Roger C. Hedlund

Ames Research Center
Moffett Field, Calif.

NATIONAL AERONAUTICS AND SPACE ADMINISTRATION • WASHINGTON, D. C. • APRIL 1967

NASA TN D-3933

THE STRUCTURE OF AN ATMOSPHERE FROM ON-BOARD MEASUREMENTS OF PRESSURE, TEMPERATURE, AND ACCELERATION

By Simon C. Sommer, Alfred G. Boissevain,
Layton Yee, and Roger C. Hedlund

Ames Research Center
Moffett Field, Calif.

NATIONAL AERONAUTICS AND SPACE ADMINISTRATION

For sale by the Clearinghouse for Federal Scientific and Technical Information
Springfield, Virginia 22151 – CFSTI price $3.00

THE STRUCTURE OF AN ATMOSPHERE FROM ON-BOARD MEASUREMENTS OF PRESSURE, TEMPERATURE, AND ACCELERATION*

By Simon C. Sommer, Alfred G. Boissevain, Layton Yee, and Roger C. Hedlund

Ames Research Center

SUMMARY

A method has been developed for determining the structure of a planetary atmosphere from measurements of pressure, temperature, and acceleration made on board an entry vehicle. Determination of the average molecular weight of the atmosphere is an important by-product of this type of measurement. Data obtained from drop tests of instrumented capsules into the Earth's atmosphere from high altitude have been analyzed. The atmosphere structure and the vehicle trajectory determined from these data are in excellent agreement with those obtained from ground-based observations and meteorological measurements. The deduced molecular weight was within 3 percent of the average value of air.

INTRODUCTION

One of the principal objectives of the early missions to other planets is to determine the structure and composition of their atmospheres. Not only is this information of considerable scientific value in the understanding of the nature of the planets but it is of great importance to the design of future vehicles intended to land scientific payloads in operating condition. The atmosphere structure, that is, the profiles of pressure, temperature, and density with altitude, is particularly important in this latter regard since it has a first-order effect on the heating and loads experienced during the high-speed portion of an entry as well as on the terminal conditions that affect the design of retardation and impact-attenuation systems. In reference 1 it was proposed that the structure of a planetary atmosphere could be determined from the acceleration-time history of a vehicle passing through it. This idea was further developed and analyzed in references 2-5. There it was shown that, as the vehicle slowed to subsonic speeds, significant errors developed from the integration of imperfect acceleration measurements over relatively long periods of time. Thus it was concluded that the use of the accelerometer method for obtaining atmosphere structure should be confined to that portion of the atmosphere traversed at speeds greater than sonic speed.

*The principal results presented herein have been summarized in an article titled "Atmosphere Definition with a Free-Falling Probe" by Simon C. Sommer and Alfred G. Boissevain, Astronaut. Aeron., vol. 5, no. 2, Feb. 1967, pp. 50-54.

For tenuous atmospheres, such as those presently postulated for Mars, supersonic impact velocities are not difficult to achieve. However, the need for sufficient time to transmit data stored during communication blackout suggests the desirability of subsonic flight prior to impact. For the dense atmospheres postulated for Venus, on the other hand, it is likely that flight at subsonic speeds would continue for many minutes. Thus it is evident that an alternative technique for defining the atmosphere structure from data obtained during subsonic flight is necessary. In references 2 and 5 the use of subsonic measurements of pitot and static pressure and ambient temperature to define the flight-path velocity was described. However, relating that information to a history of altitude above impact to determine the atmosphere structure required a knowledge of the mean molecular weight of the gas and the variation of flight-path angle with time.

A method has been developed whereby the measurements of pressure, temperature, and acceleration can be used to determine the mean molecular weight of the gas and atmosphere structure with no prior knowledge of gas properties or trajectory information. It is the purpose of this paper to describe this method and the results of two flight tests designed to evaluate the concept and to identify the problems from actual flight-test experience. In the first test, an instrumented capsule, dropped from an aircraft flying at 37,000 feet, descended in free fall at relatively low velocities. In the second test, a capsule was balloon-launched at approximately 130,000 feet; it dropped at speeds approaching Mach number one. The conditions of the second test were designed to cover part of the velocity-density regime that would be expected in an entry into the Martian atmosphere.

We wish to acknowledge the excellent cooperation of the personnel at both the Department of Defense Joint Parachute Test Facility at El Centro, California, and at the Air Force Cambridge Research Laboratory, Holloman Air Force Base, New Mexico.

SYMBOLS

A	maximum cross-sectional area of capsule normal to axis of symmetry
a_s	aerodynamic acceleration along the flight path
C_D	drag coefficient
C_p	pressure coefficient
C_L	lift coefficient
d	maximum diameter of capsule
g	acceleration due to gravity
h	altitude above impact

M	Mach number
$\dot{m}$	mass of capsule
p	pressure
q	dynamic pressure, $\frac{1}{2}\rho V^2$
R	gas constant for air, $\frac{\text{universal gas constant}}{\text{molecular weight}}$
r	distance between center of planet and capsule
T	temperature
t	time
V	velocity of capsule relative to surrounding gas
γ	ratio of specific heats
θ	flight-path angle, measured from local horizontal, positive down
ρ	atmospheric density

Subscripts

f	final conditions at impact
i	first measured value
t	stagnation values

ANALYSIS

The problem to be solved is the determination of the state properties of the atmosphere as functions of altitude above ground level from on-board measurements of temperature and pressure at points within the flow field of the descending probe, and three components of acceleration of the probe center of gravity. The determination of the temperature and pressure require only that the values measured be corrected for vehicle angle of attack and flow field effects which in turn require definition of the probe attitude and Mach number at the times of measurement. Determining the density requires, in addition, that the gas constant be known or evaluated. Furthermore, the probe altitude above impact must be determined as a function of time so that the state properties of the atmosphere can be related to altitude. The analysis which follows derives equations for applying the on-board measurements to the definition of these quantities.

Altitude can be determined from free-stream pressure and density by means of the barometric equation

$$dp = -\rho g dh \tag{1}$$

and the equation of state

$$p = \rho RT \tag{2}$$

to obtain

$$dh = -\frac{R}{g}\frac{T}{p}dp \tag{3}$$

If it is assumed that g is constant during the terminal portion of the flight, equation (3) can be integrated to give

$$h = \frac{R}{g}\int_{p}^{p_f}\left(\frac{T}{p}\right)dp \tag{4}$$

where h is the altitude above impact.

Since T and p are measured quantities, and it is assumed that the value of g is known, the value of gas constant must be known or evaluated in order to determine the altitude above impact. When R is unknown, the following analysis can be used.

The balance of forces along a trajectory of a capsule entering a spherically symmetric nonrotating planetary atmosphere can be written as follows:

$$\frac{1}{g}\frac{dV}{dt} + \frac{1}{g}\left(\frac{C_D A}{m}\right)\left(\frac{1}{2}\rho V^2\right) - \sin\theta = 0 \tag{5}$$

which can be rewritten as

$$C_D\left(\frac{1}{2}\rho V^2\right)A = ma_s \tag{6}$$

where a_s is the component along the flight path of aerodynamic acceleration deduced from accelerometer measurements.

The rate of change of altitude with time is given by

$$dh = -(V \sin\theta)dt \tag{7}$$

Combining equations (3) and (7) gives

$$V = \frac{R}{g}\frac{T}{p}\frac{1}{\sin\theta}\frac{dp}{dt} \tag{8}$$

If equation (6) is combined with equations (2) and (8), V can be eliminated as follows:

$$V = \left[\left(\frac{2m}{C_D A}\right) a_s R \left(\frac{T}{p}\right)\right]^{1/2} = \frac{R}{g}\frac{T}{p}\frac{1}{\sin\theta}\frac{dp}{dt} \tag{9}$$

from which

$$\frac{dp}{dt} = \sin\theta\left[\left(\frac{2m}{C_D A}\right) g^2 a_s \left(\frac{p}{T}\right)\frac{1}{R}\right]^{1/2} \tag{10}$$

and

$$R = \frac{(2m/C_D A)g^2(\sin^2\theta)a_s(p/T)}{(dp/dt)^2} \tag{11}$$

For the purpose of this analysis, it is assumed that the drag coefficient, C_D, mass, m, and frontal area, A, are known from previous measurements. In equation (11), the only quantity that is not known or measured is the flight-path angle, θ. In order to determine flight-path angle, the equation for the instantaneous balance of forces normal to a trajectory of a capsule entering the atmosphere is required.

$$\frac{V}{g}\frac{d\theta}{dt} + \left(\frac{V^2}{gr} - 1\right)\cos\theta + \frac{1}{g}\frac{C_L A}{m}\left(\frac{1}{2}\rho V^2\right) = 0 \tag{12}$$

If it is assumed that $V^2/gr \ll 1$, as is the case for the terminal portion of a trajectory, equation (12) reduces to

$$\frac{V}{g}\frac{d\theta}{dt} - \cos\theta + \frac{1}{g}\frac{C_L A}{m}\left(\frac{1}{2}\rho V^2\right) = 0 \tag{13}$$

Substituting for $(1/2)\rho V^2$ and V from equations (6) and (8), respectively, and solving for R, we find

$$R = \frac{\{g\cos\theta - [(C_L/C_D)a_s]\}g\sin\theta(p/T)}{(d\theta/dt)(dp/dt)} \tag{14}$$

If R is eliminated between equations (11) and (14) in order to solve for θ, then

$$\left[g \cos \theta - \left(\frac{C_L}{C_D} a_s\right)\right] \frac{dp}{dt} = \left(\frac{2m}{C_D A} g a_s \sin \theta\right) \frac{d\theta}{dt} \tag{15}$$

With the substitution

$$\left.\begin{aligned} \cos \theta &= y \\ -\sin \theta \, d\theta &= dy \end{aligned}\right\} \tag{16}$$

Equation (15) becomes

$$\frac{dy}{dp} + \left[\frac{1}{(2m/C_D A)a_s}\right] y = \frac{C_L/C_D}{(2m/C_D A)g} \tag{17}$$

Equation (17), a linear differential equation of the first order, is solved by substituting equation (16) and evaluating the constant of integration to obtain

$$\cos \theta = \left\{\int_{p_i}^{p} \frac{C_L/C_D}{(2m/C_D A)g} \exp\left[\int_{p_i}^{p} \frac{dp}{(2m/C_D A)a_s}\right] dp + \cos \theta_i\right\} \exp\left[-\int_{p_i}^{p} \frac{dp}{(2m/C_D A)a_s}\right] \tag{18}$$

Equation (18) gives the flight-path angle, θ, as a function of an initial value, θ_i, and measured parameters. Since it must be assumed that θ_i is not known, equation (11) is used in the following form:

$$\cos \theta = \left[1 - \frac{(dp/dt)^2 R}{(2m/C_D A)g^2 a_s (p/T)}\right]^{1/2} \tag{19}$$

to replace $\cos \theta$ and $\cos \theta_i$ by the expression that contains the single desired unknown, R. This substitution yields the following expression

$$\left[1 - \frac{(dp/dt)^2 R}{(2m/C_D A)g^2 a_s (p/T)}\right]^{1/2} = \left\{\int_{p_i}^{p} \frac{C_L/C_D}{(2m/C_D A)g} \exp\left[\int_{p_i}^{p} \frac{dp}{(2m/C_D A)a_s}\right] dp + \left[1 - \frac{(dp/dt)_i^2 R}{(2m/C_D A)_i g^2 a_{s_i} (p/T)_i}\right]^{1/2}\right\} \exp\left[-\int_{p_i}^{p} \frac{dp}{(2m/C_D A)a_s}\right] \tag{20}$$

where m/C_DA has been treated as variable to allow for transonic and subsonic variations in C_D. Evaluating the gas constant, R, from equation (20) now allows the altitude history to be determined from equation (4). It is now possible to relate pressure, temperature, and density (from eq. (2)) to the deduced altitude. In addition, velocity and flight-path-angle histories can be determined.

Special Case of $C_L = 0$

When $C_L = 0$, equation (13) reduces to

$$\cos \theta = \frac{V}{g} \frac{d\theta}{dt} \tag{21}$$

equation (18) reduces to

$$\frac{\cos \theta}{\cos \theta_i} = \exp\left[- \int_{p_i}^{p} \frac{dp}{(2m/C_DA)a_s} \right] \tag{22}$$

and equation (20) reduces to

$$R = \frac{1 - \exp\left[- \int_{p_i}^{p} \frac{dp}{(m/C_DA)a_s} \right]}{\frac{(dp/dt)^2}{(2m/C_DA)g^2a_s(p/T)} - \left[\frac{(dp/dt)_i^2}{(2m/C_DA)_i g^2 a_{s_i} (p/T)_i} \right] \exp\left[- \int_{p_i}^{p} \frac{dp}{(m/C_DA)a_s} \right]} \tag{23}$$

Special Case, $C_L = 0$, $\theta = 90^\circ$

For the case of vertical entry into a planetary atmosphere, or for a portion of the trajectory where $\theta = 90^\circ$, equation (11) reduces to

$$R = \frac{(2m/C_DA)g^2a_s(p/T)}{(dp/dt)^2} \tag{24}$$

and all trajectory parameters can be evaluated. For this special case, an alternate solution for determining the gas constant, R, can be derived. Equation (10) with $\sin \theta = 1$ becomes

$$\frac{dp}{dt} = \left[\left(\frac{2m}{C_D A}\right) g^2 a_s \left(\frac{p}{T}\right) \frac{1}{R}\right]^{1/2} \tag{25}$$

from which

$$\int_p^{p_f} \frac{dp}{p^{1/2}} = \frac{g}{R^{1/2}} \int_t^{t_f} \left[a_s \left(\frac{2m}{C_D A}\right) \frac{1}{T}\right]^{1/2} dt \tag{26}$$

integrating equation (26) and solving for R gives

$$R = g^2 \left\{ \frac{\int_t^{t_f} [a_s(2m/C_D A)(1/T)]^{1/2} dt}{2(p_f^{1/2} - p^{1/2})} \right\}^2 \tag{27}$$

The advantage of using equation (27) instead of equation (24) is that integrating measured data is more accurate than differentiating the same data. For the experiments that will be reported herein, the gas constant, R, was determined from equation (27).

Determination of Free-Stream Conditions

The analysis presented above has been based on a knowledge of free-stream pressures and temperatures. In practice, the measured pressures will be affected by both angle of attack and flow compressibility. Angle of attack can be determined by use of measured values of lateral and axial acceleration in combination with wind-tunnel measurements of vehicle aerodynamics. Pressures can then be corrected to stagnation values by use of wind-tunnel pressure distributions. Stagnation temperatures can be measured directly with properly designed temperature probes.

The process of converting stagnation values of pressure and temperature to free-stream values will, of course, be an iterative one. The aerodynamic and pressure coefficients necessary for correcting measured pressure to stagnation pressure are functions of Mach number which are unknown until the data are processed. The equations given below provide the basis for the iteration. Ideal gas equations are assumed to be applicable.

From equation (6),

$$\left.\begin{aligned} q &= (m/C_D A) a_s \\ \text{and} \qquad q &\equiv (1/2)\rho V^2 = (\gamma/2) p M^2 \end{aligned}\right\} \tag{28}$$

Solving for p gives

$$p = \frac{(m/C_D A)a_s}{(\gamma/2)M^2} \tag{29}$$

Now, since

$$\frac{p_t}{p} = \left(1 + \frac{\gamma - 1}{2} M^2\right)^{\gamma/(\gamma-1)} \tag{30}$$

Then

$$\frac{p_t}{q} = \frac{p_t}{(m/C_D A)a_s} = \frac{\{1 + [(\gamma - 1)/2]M^2\}^{\gamma/(\gamma-1)}}{(\gamma/2)M^2} \tag{31}$$

Equation (31) allows for the evaluation of Mach number in terms of measured parameters if the value of γ is known. Except for the Earth's atmosphere, it is likely that γ will not be reliably known; however, γ has only minor effects on the determination of atmosphere properties so an estimate from best available information can be used. This will be demonstrated in a later section. With γ assumed and Mach number evaluated from equation (31), free-stream pressure can then be evaluated from equation (29) or (30). Free-stream temperature can now be evaluated by use of

$$\frac{T_t}{T} = 1 + \frac{\gamma - 1}{2} M^2 \tag{32}$$

EXPERIMENTS

Two flight tests were made to evaluate the foregoing analysis. In the first test, a modified spherical capsule was dropped from an aircraft flying at approximately 37,000 feet (11.28 km) and fell at relatively low velocities. In the second test, the configuration was changed to a modified blunted cone which was released from a balloon at an altitude of approximately 130,000 feet (39.62 km).

The second test, which included the altitude regime of the first, will be discussed in the following sections. A complete description of the model used in the second test, including its construction and instrumentation, can be found in appendix A. Also found in this appendix is a description of the balloon-launch system. Appendix B contains a complete resumé of the airplane drop test.

MODEL AND INSTRUMENTATION

The model for the balloon drop test was a 55° half-angle round-nosed cone with a conical afterbody. It weighed 37 pounds (16.78 kg) and had a diameter of 30.5 inches (0.77 m). A drawing of the model (fig. 1(a)) shows the location of each orifice for the pressure transducers, the position of each temperature transducer, and the center of gravity (the position of the effective center of pendulous mass of three mutually perpendicular linear accelerometers).

One vibrating-diaphragm pressure transducer, developed at Ames Research Center, was located at the center of the model face (i.e., stagnation point for zero angle of attack), p_1, and one at the beginning of the conical section of the forebody, p_3. This novel transducer is described in detail in reference 6. Three commercially available unbonded strain-gage pressure cells were located at p_1, p_2 (180° from p_3), and p_4 (the instep of the afterbody). Two commercially available platinum resistance temperature transducers in different configurations were located at positions T_1 and T_2 on the conical forebody. A photograph of the assembled model is shown in figure 1(b). Note the two temperature transducers protruding through the surface.

The temperature transducers were installed outside the boundary layer, thus avoiding the measurement of a temperature influenced by convective transfer from the body surface. Moreover, the transducers were surrounded by metallic enclosures (of two different designs) to minimize the effects of radiative transfer from the model, the Earth, and the sun.

Calibration and Accuracy

The pressure and temperature transducers were calibrated on the ground with their appropriate telemetry oscillators to give calibration curves in terms of frequency versus the measured property. The pressure sensors were calibrated against Bourdon tube gages through a range from 1 to 760 mm Hg. The temperature sensors were placed in a thermal chamber and calibrated against mercury thermometers from -60° to +60° C. The voltage output of the mounted accelerometers was measured as a function of static attitude and combined with the known transfer functions of the accelerometer oscillators to provide calibration curves of output frequency versus acceleration for each accelerometer. The oscillators, pressure transducers, and accelerometers were at room temperature during calibration. The accuracy of the calibration as determined by the repeatability of measurements is as follows: pressure, a fraction of 1 mm Hg; temperature, less than 1° C; and acceleration, 0.005 g. However, the calibration errors are considered small when compared with the errors introduced by the data transmission. The accuracy of the data processed through the transmission system is estimated to be no better than 2 percent of the reading.

RESULTS AND DISCUSSION

The balloon test was conducted at the White Sands Missile Range, New Mexico, under the sponsorship of the Air Force Cambridge Research Laboratory. AFCRL was responsible for balloon-launched operations, and WSMR was responsible for data acquisition, radar tracking, and meteorological information.

A 10-channel FM-FM telemetry unit transmitted continuous real-time records of pressures, temperatures, and aerodynamic acceleration of the model from 10 minutes prior to capsule release to impact. The ground-based radar measured the actual capsule trajectory during descent. Radiosonde balloons and sounding rockets measured the atmospheric structure a few hours before and after the drop to provide information to compare with the atmospheric properties deduced from on-board measurements.

Measured Data

Figure 2 shows the variations of the measured properties as functions of time after capsule release. The data were continuous in nature but, for convenience, are shown as discrete points in this and subsequent figures. Values of pressure, in millibars, of three transducers presenting credible data are shown in figure 2(a). The results from one of the Ames vibrating-diaphragm cells, at the stagnation point, p_1, were at significant variance with pressures measured by the other cells where the recording ranges overlapped; these values are therefore not shown. The instrument calibration section of appendix A includes a discussion of the possible cause of this discrepancy. In addition, one of the telemetry subcarrier oscillators in the strain-gage cell system, measuring pressures at p_2, malfunctioned prior to launch. A reliable calibration with a substitute oscillator was not made and therefore the data from this cell also are omitted.

Of the other pressure transducers, note that only the Ames vibrating-diaphragm cell, at p_3, was sensitive enough to measure the low pressures encountered in the initial portion of the trajectory. This particular transducer reached its design limit (250 mb) at about 265 seconds after release. The strain-gage pressure transducer at p_1 had a minimum threshold of about 14 mb ($t = 45$ sec) and the strain-gage pressure transducer at p_4 had a minimum threshold of about 23 mb ($t = 75$ sec). These latter gages subsequently gave continuous readings until capsule impact.

Figure 2(b) shows the variation of measured recovery temperature (for these conditions, essentially equivalent to stagnation temperature) from the time of capsule release to impact as given by the two temperature transducers mounted at T_1 and T_2. For approximately 2 hours before the capsule was released, the balloon-capsule system was at an altitude of over 120,000 feet (36.58 km), drifting toward the drop area with very little airflow passing through the temperature transducers. During this time, the capsule and temperature transducers had reached an equilibrium temperature of approximately 297° K. The free-stream temperature measured by meteorological

soundings was 240° K. The difference between these two values can be attributed to the solar radiation incident on the capsule support and shield and the Earth's albedo incident on the transducers themselves. The reasons for the discrepancy between the two transducers during descent are not known, and a simple average of the two readings was used in the data analysis with no correction for the initial high value of temperature.

Figure 2(c) shows the variation of aerodynamic acceleration as a function of time for the duration of the flight. Note the change in time scale at 100 seconds. Since the angular excursions were estimated to be small during the entire flight, the values of aerodynamic acceleration shown in the figure can be considered to be the pathwise aerodynamic acceleration, a_s.

Data Analysis

The p_3 and p_4 values of pressure shown in figure 2(a) were corrected to stagnation values as a means of obtaining an average variation of pressure with time for use in the subsequent analysis of the data for atmospheric reconstruction. The method used is described in the following paragraphs.

From the definition of pressure coefficient, C_p, the following expression can be obtained

$$p_t = p_n + q(C_{p_t} - C_{p_n}) \tag{33}$$

where the subscript t refers to stagnation values and n refers to the appropriate body location of pressure measurement. The variation of C_p with Mach number was obtained for the several sensor locations from unreported tests of this model configuration in the Ames 12-Foot Pressure Wind Tunnel, and are summarized here in figure 3.

An initial calculation of Mach number as a function of time was determined from equation (31) using measured values of a_s and values of measured pressure assumed to be stagnation values. Values of dynamic pressure, q, were calculated using equation (28) allowing an initial correction to be made to the measured values of pressure in equation (33). This process was repeated until equation (31) showed the change in calculated Mach number at a given time to be small.

The drag coefficient, C_D, used throughout the data reduction was assumed constant at a value of 0.91. This value was obtained from unpublished tests made in one of the Ames ballistic facilities at a Mach number of approximately 0.7. To ascertain the effects of using a variable C_D in the data reduction, an assumed variation of C_D with Mach number did not yield results that were appreciably different from those obtained with C_D as a constant.

The values of stagnation pressure computed from other orifice locations agreed well with those measured at the stagnation point, p_1. The average value of stagnation pressure as a function of time used in the analysis of

atmospheric reconstruction is shown in figure 4. The maximum variance of the three stagnation pressures at any given time was ±3 percent of the average value. It should be noted that with the same basic information, it is possible to correct the measured values of pressure to free-stream values. For convenience in data reduction, the above procedure was used.

The average values of p_t and Mach number as functions of time were then used with equations (30) and (32) to find free-stream pressure and temperature as functions of time.

Trajectory Reconstruction

The special case in which $C_L = 0$ and $\theta = 90^\circ$ was used for reconstructing the trajectory; this allowed the use of equation (27) for the evaluation of the gas constant, R. The value of molecular weight of the air, obtained from the evaluation of R, was 29.83, which was 3 percent higher than the accepted value of 28.96. The altitude above impact as a function of time was evaluated by the use of equation (4), and is compared to the actual trajectory as obtained from radar tracking in figure 5. The altitude at impact was 4175 feet (1.27 km) above mean sea level, and is shown as the termination at 538 seconds after capsule release. Agreement between deduced and actual altitude is considered excellent.

Model velocity was evaluated from equation (9) and is shown in figure 6 as a function of deduced altitude. These values are compared to those obtained from radar tracking. The agreement is considered satisfactory.

Atmosphere Reconstruction

The deduced atmosphere structure, as determined from the on-board measurements only, is shown in figure 7. Figure 7(a) shows the deduced free-stream pressure as a function of deduced altitude and is compared with radiosonde meteorological measurements. Agreement between deduced and measured pressure is excellent.

Figure 7(b) presents free-stream temperature as a function of deduced altitude, and is again compared with the radiosonde data. The large difference between deduced and free-stream temperatures at the highest altitude can be attributed to the initial high temperature of the capsule and transducers just prior to capsule release. In the altitude range from about 100,000 feet (30.48 km) to 40,000 feet (12.19 km) the radiosonde-measured values are less than the deduced values by about 15° C. No explanation can be given for this discrepancy, although it is presumed to be due to incomplete thermal isolation of the sensors on either the radiosonde or the probe.

Figure 7(c) shows the deduced free-stream density (from eq. (2)) as a function of deduced altitude. There is good agreement between deduced and measured free-stream density.

Effects of γ on Atmosphere Structure

A value of $\gamma = 1.4$ was used for evaluating the results of the preceding sections. In order to determine the effects of uncertainty in γ, the basic data were also analyzed using values of γ of 1.2 and 1.6. The effects of these extreme values on atmosphere structure is small as shown in figure 8, where deduced density is plotted as a function of deduced altitude. The effects of γ on both p and T were similarly small. The evaluation of the gas constant, R, was essentially unaffected by the changes in γ, for R changed by only ±0.3 percent.

If real gas equations were used to relate the thermodynamic properties to flight conditions in equations (28) through (32), that is, if γ were allowed to change during terminal flight (see ref. 7), it is expected that equally small effects on atmosphere structure would be obtained.

Simulated Martian Entry

In order to simulate the terminal phase of an entry into the Martian atmosphere this flight was assumed to have terminated at an impact altitude of about 101,000 feet (30.78 km), corresponding to a surface pressure of a little over 11 mb. This was equivalent to terminating the present test 50 seconds after the drop. A complete analysis of the data was then made over this portion of the trajectory. Some of the important results of this analysis are summarized in figure 9, which presents the deduced altitude above assumed impact as a function of time, and in figure 10, which shows the free-stream density as a function of deduced altitude. In both of these figures comparison is made with ground-based observations. The general agreement between deduced and measured properties is still considered acceptable, although the prediction of density at the higher altitude is not as good as that computed from the entire flight, showing a maximum error of 14 percent. The value of molecular weight computed from this short-term evaluation of R was 31.40, almost 8 percent higher than the accepted value of 28.96. The nature of the tests and the instrumentation was such that the relative accuracy of property measurement was far higher at low altitudes than at the beginning of the flight in the region of low ambient pressures and starting transients of free fall. Better matching of the instruments to these atmospheric conditions should improve the data.

CONCLUDING REMARKS

An analysis has been developed for determining the atmosphere structure, the mean atmospheric molecular weight, the velocity-altitude history, and the flight-path-angle history of a descending probe in low speed flight from onboard measurements of pressure, temperature, and acceleration. The determination of the average molecular weight of the atmosphere is an important result of this analysis.

The technique has been demonstrated by analyzing data obtained from drop tests of instrumented capsules into the earth's atmosphere from high altitude. The atmosphere structure and the vehicle trajectory determined from these data agree well with those obtained from ground-based observations and radiosonde meteorological measurements. The deduced molecular weight, for example, was within 3 percent of the accepted value for air. It should be noted that in the experiments described, the capsule descent was vertical except for wind drift, thus simplifying the determination of the molecular weight. Although it has not yet been demonstrated that data from a flight other than vertical would yield equally satisfactory results, methods for analyzing this case have also been described.

Ames Research Center
National Aeronautics and Space Administration
Moffett Field, Calif., 94035, Jan. 31, 1967
124-07-02-25-00-21

APPENDIX A

ADDITIONAL DESCRIPTION OF BALLOON DROP MODEL AND TEST

Model Description

The capsule forebody was constructed of 3/8-inch (9.5 mm) thick end-grain balsa wood blocks sandwiched between two layers of 1/64-inch (0.4 mm) thick glass fiber. A hardwood hoop at the major diameter insured structural rigidity. The forebody was filled with a preshaped plastic foam form glued in place with polyester resin and was cut out to receive the instruments. The plastic foam was coated with latex paint to minimize crumbling during handling.

The afterbody was constructed of 1/32-inch (0.8 mm) thick glass fiber reinforced at the maximum diameter with plywood. In addition, four reinforcing glass fiber longerons were installed on the inside conical surface of the afterbody to prevent buckling. The pressure transducers were mounted near the plane of maximum diameter and were connected to the orifices by 1/8 inch O.D. copper tubing. The capsule was designed to fail progressively upon impact for instrument survival.

Ballast was used to fix the center of gravity at the desired location and to equalize the moments of inertia about the two transverse axes.

The center of gravity was originally placed at the intersection of the major diameter plane and the model axis. To test for dynamic stability, a mock-up of the model with this center-of-gravity location was dropped, with an initial angle of attack of 30°, from a helicopter at about 2000-foot (610 m) altitude. In a classic demonstration of dynamic instability, the falling model oscillated with increasing pitch angle until it tumbled about 200 feet (61 m) above impact.

An identical model, with the center of gravity moved forward by 1.25 inches (3.18 cm) (i.e., 4 percent of d) and dropped under similar conditions, damped out after several cycles and descended to the ground at essentially 0° angle of attack.

Instrumentation

A 10-channel standard IRIG FM-FM telemetry system transmitted measured properties to ground stations during the flight. The telemetry system consisted of a transmitter, a mixer-amplifier, 10 subcarrier voltage-controlled oscillators (2.3 through 40 kc), and their associated circuitry. The telemetry and instrumentation system is shown in a block diagram in figure 11. The system provides for checking the calibration in flight. The calibration sequence was initiated each time the transmitter was turned on.

The location of the transducers and TM equipment in the forebody are shown in figure 12. The afterbody and a metallic R.F. shield over the transmitter unit are not shown.

The internal configuration of the accelerometers was such that the axis about which these units were insensitive to angular rate and angular acceleration was located outside of the case, typically by about one inch. This position was experimentally determined for each accelerometer and each unit was mounted such that this point was located on the model center of gravity. Thus each accelerometer would respond to linear accelerations of the model center of gravity along its sensitive axis only.

A four-way corner reflector, constructed of thin copper sheet and filled with plastic foam, was installed beneath the transmitter chassis to aid the radar in acquiring the capsule after its release from the balloon.

The assembled capsule was placed in an altitude-temperature chamber programmed to simulate the altitude-time history of the expected balloon ascent. Thermocouples were placed at various points on and in the capsule. All areas of the capsule and instrumentation followed the ambient temperature with the exception of the transmitter chassis. This unit maintained its normal operating temperature of about 40° C. It should be noted that the transmitter was turned on at selected times during the simulated flight. Calibrations of the pressure sensors were then made in the altitude-temperature chamber at the low ambient temperatures expected during the flight. The only pressure sensor that showed a significant variation of calibration with temperature was the Ames vibrating-diaphragm cell system connected to the orifice at the center of the forward face, p_1. During the actual flight, as was discussed in the text, the soak temperature of the capsule was far higher than the ambient temperature of the air, so that the calibrations made in the cold chamber were not applicable. Neither the room temperature calibration nor the cold-chamber calibration for the vibrating-diaphragm sensor at p_1 gave reasonable values of pressure. The most probable explanation for this discrepancy is that the temperature of the sensor system inside the capsule was different from the temperatures for which calibrations were available.

Capsule-Balloon Interface

During the 5-hour flight from balloon launch to the time of capsule release the capsule was suspended in a tubular hanger that contained an external battery for power and associated control circuits for the operation of the capsule. This unit, with the capsule in place, but without a thin mylar sheet radiation shield, is shown in figure 13. The capsule was suspended from the top of the hanger with a 7-strand aircraft cable which fed through two explosive cable cutters not visible under the disk.

Four ground-controlled radio commands were available through the balloon system for controlling the capsule during ascent. One of these commands was used to fire the explosive cable cutters. The three other commands were

used to turn the transmitter on or off, or to switch from external to capsule power. The commands were momentary and could be used only one at a time. The block diagram for these control functions is shown in figure 14.

Balloon Operation

The balloon system just before launch and just after launch is shown in figures 15(a) and 15(b). The package on the right end of the beam beneath the balloon and parachute is the hanger with capsule in place. The packages at the center of the beam contained batteries and support electronic equipment for the balloon operation. The package at the left end of the beam contained a radio-controlled ballast box. The beam was connected to a deployed parachute which was attached with an explosive bolt to the base of the balloon.

The balloon was "flown" from the launch site to the drop area at the desired altitude by taking advantage of the prevailing winds and by controlling the ascent rate. The control of the ascent rate was achieved through valving excess helium or releasing ballast. A map showing the balloon trajectory is presented in figure 16. A half hour after the capsule was released the control equipment was cut loose from the balloon and recovered by the parachute.

The recovered capsule is shown in figure 17. The concentric ring failures coincided with the joints of the balsa wood blocks used in the sandwich construction of the capsule forebody. The two temperature sensors are visible. The capsule impacted in loosely packed sand at a velocity of about 90 ft/sec (27.4 m/sec).

As a matter of interest, the capsule, just prior to impact, was observed to be rotating at about 6 rpm about its longitudinal axis. This was determined from the variation of signal strength of the telemetered signal as received at the ground station.

APPENDIX B

AIRPLANE DROP EXPERIMENT

The first experimental test of the atmosphere-probe program consisted of dropping a ring-stabilized sphere from an airplane at an altitude of 37,000 feet (11.3 km). Time histories of model surface pressure, total temperatures, and model acceleration were obtained from telemetered data.

Model and Instrumentation

The instrumentation was similar to that already described except that the Ames vibrating-diaphragm pressure transducers were not used. Unbonded strain-gage pressure cells were used throughout. In two places differential-pressure cells were used, with the center of capsule face as the reference pressure.

A sketch of the model used in this test is shown as figure 18(a). A photograph of the assembled model is shown in figure 18(b). The basic sphere was constructed of 1/16-inch (1.6 mm) thick glass fiber. The stabilizing ring was made of foam covered with glass fiber.

The need for a stabilizing ring was clearly established in drops of noninstrumented models made to verify the operation of a recovery parachute. The motions of the sphere were erratic and violent with angular excursions reaching 90° angle of attack and roll rates of up to 5 revolutions per second. Data on these angular excursions were obtained from analysis of film from a 16-mm gun camera aimed along the axis of symmetry of the model and through a small glass port at the nose.

The model was dropped from the bomb-bay of an RB-66. A holder in the bomb-bay held the model in a horizontal position. Drop was initiated by firing a squib which released some restraint straps. A spring-activated plate helped to thrust the model down and into the free flow field around the airplane. The model was tracked by ground-based cameras to determine its trajectory. A barostat-operated switch activated a parachute recovery system at an altitude of about 8000 feet (2.44 km).

Experimental Data

The model achieved vertical flight after 20 seconds of flight, and recovery sequence was initiated approximately 160 seconds after launch. The data obtained during this portion of the flight are shown in figure 19.

The pressures shown in figure 19(a) are a composite of the outputs from the three absolute pressure cells. The pressure difference between the two differential cells was too small to be measured under the conditions of

flight. The absolute pressure cells gave readings that had similar variation with time, but were displaced from one another. It was determined after the flight that the type of physical mounting of the pressure cells in the model, was such that the cases were deformed, producing a bias to the readings. For purposes of analysis the readings of the three cells at a time of 1 second after launch were brought to a common ambient pressure at that altitude as determined by radiosonde measurements. The experimental values of pressure as a function of time, as used in the analysis and shown in figure 19(a), were the simple arithmetic mean of the values of the three cells at any given time, corrected for the bias error as described.

The variation of measured temperature with time is shown in figure 19(b). The values of temperature used in the analysis were the mean of the two measured values, shown in this figure.

The total acceleration variation with time is shown in figure 19(c). The starting transients of launch are over by 20 seconds and the model is effectively in vertical flight. Note the high initial deceleration upon insertion of the model in the relatively high velocity flow (about 450 ft/sec) (137 m/sec) upon release from the aircraft.

The traces of accelerometer output showed high-frequency disturbances of up to 0.2 g. These were interpreted as the effect of buffeting which is a typical characteristic of this class of blunt bodies at subsonic speeds. Care must be exercised in selecting a configuration, the mounting of instruments, and the sampling of data to minimize buffeting and its effects, for this type of forcing function can interfere with and degrade the measurement of aerodynamic acceleration.

RESULTS

The pressure and temperature (both assumed to be free-stream values as measured in view of the low Mach numbers) and total acceleration as functions of time were analyzed in the manner described for the balloon drop test in the body of the report. A drag coefficient of 0.814, evaluated from the analysis of ground-tracking data, was used in the data reduction. The results of the analysis are summarized in figure 20, which shows the reconstruction of the model trajectory in terms of altitude as a function of time and shows the observed trajectory for comparison. Figure 21 is the atmosphere structure as deduced from the analysis and is compared to radiosonde values taken at the time of the test. Pressure in millibars, as a function of deduced altitude, is shown in figure 21(a). The variation of temperature with deduced altitude is shown in figure 21(b), and density, also as a function of deduced altitude, is shown in figure 21(c). The deduced value of the gas constant, R, yielded a value of 29.06 for the molecular weight of air, 0.3 percent higher than the average accepted value of 28.96.

REFERENCES

1. Seiff, Alvin: Some Possibilities for Determining the Characteristics of the Atmospheres of Mars and Venus From Gas-Dynamic Behavior of a Probe Vehicle. NASA TN D-1770, 1963.

2. Seiff, Alvin; and Reese, David E., Jr.: Defining Mars' Atmosphere - A Goal for the Early Missions. Astronaut. Aero., vol. 3, no. 2, Feb. 1965, pp. 16-21.

3. Peterson, Victor L.: A Technique for Determining Planetary Atmosphere Structure From Measured Accelerations of an Entry Vehicle. NASA TN D-2669, 1965.

4. Peterson, Victor L.: Analysis of the Errors Associated with the Determination of Planetary Atmosphere Structure From Measured Accelerations of an Entry Vehicle. NASA TR R-225, 1965.

5. Seiff, Alvin; and Reese, David E., Jr.: Use of Entry Vehicle Responses to Define the Properties of the Mars Atmosphere. AAS Preprint 65-24, 1965.

6. Southwest Research Institute: Vibrating Diaphragm Pressure Transducer. NASA Technology Utilization Report, SP-5020, 1966.

7. Peterson, Victor L.: Equations for Isentropic and Plane Shock Flows of Mixtures of Undissociated Planetary Gases. NASA TR R-222, 1965.

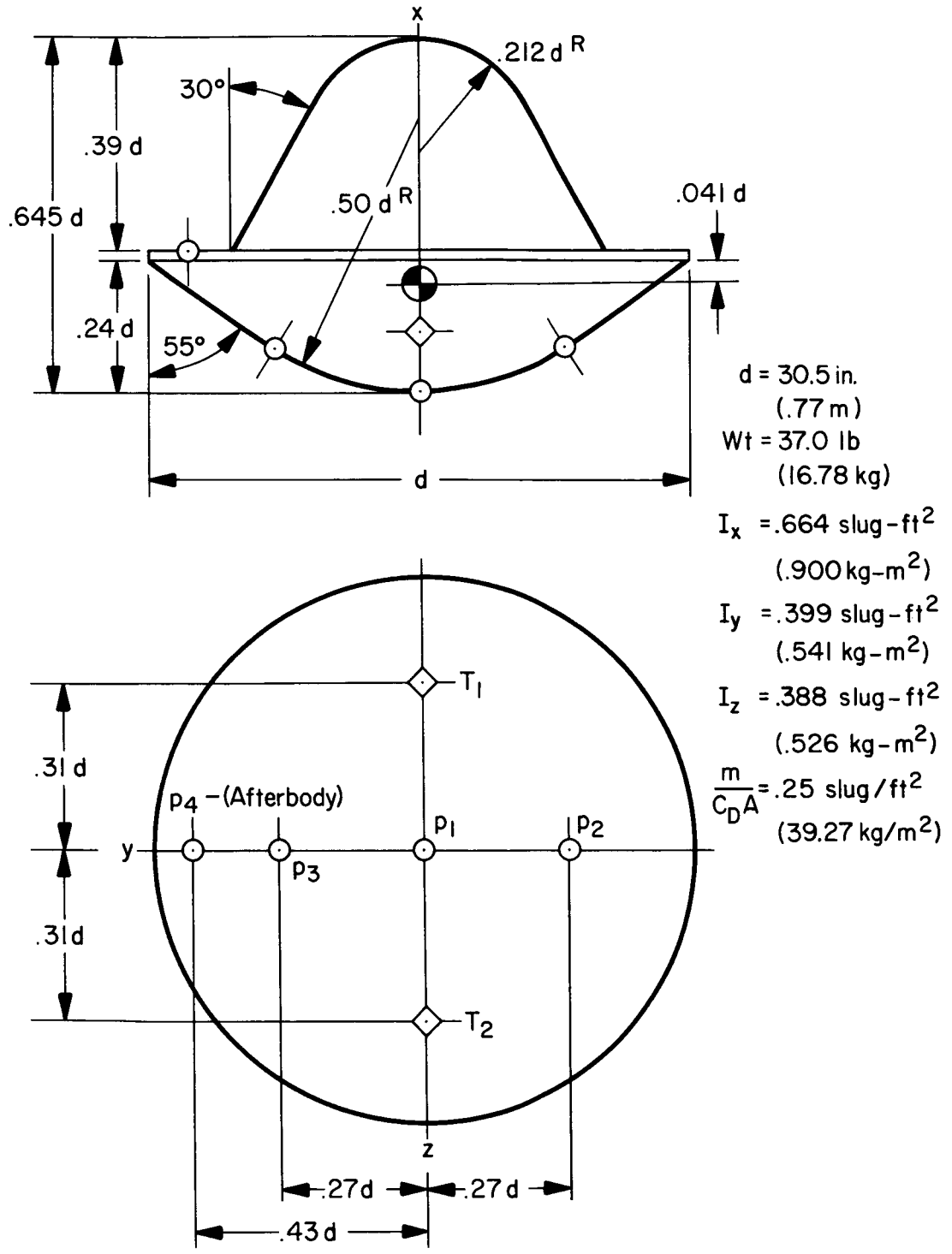

(a) Sketch and physical dimensions.

Figure 1.- Conical model for balloon experiment.

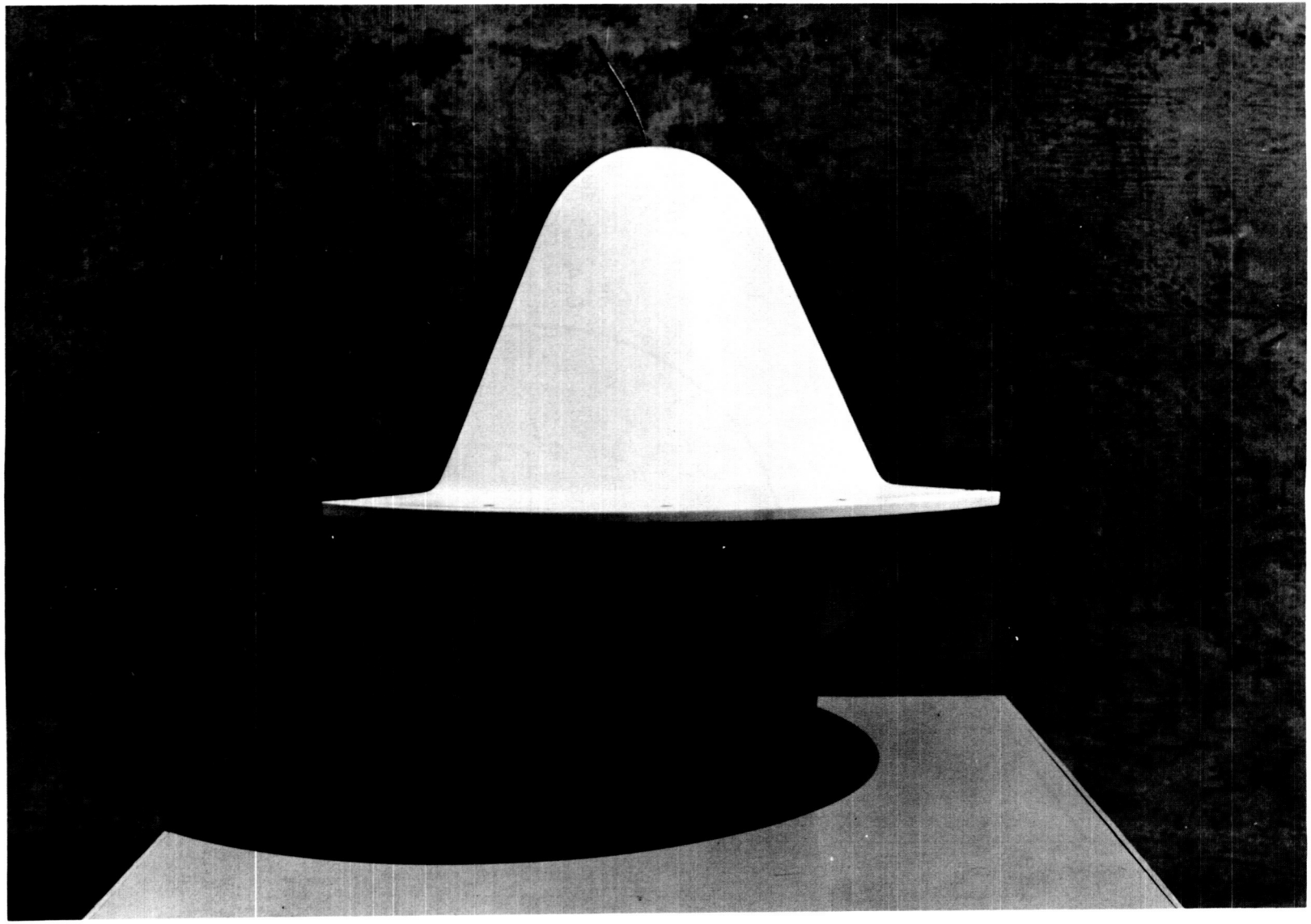

A-37054-7

(b) Photograph of assembled model.

Figure 1.- Concluded.

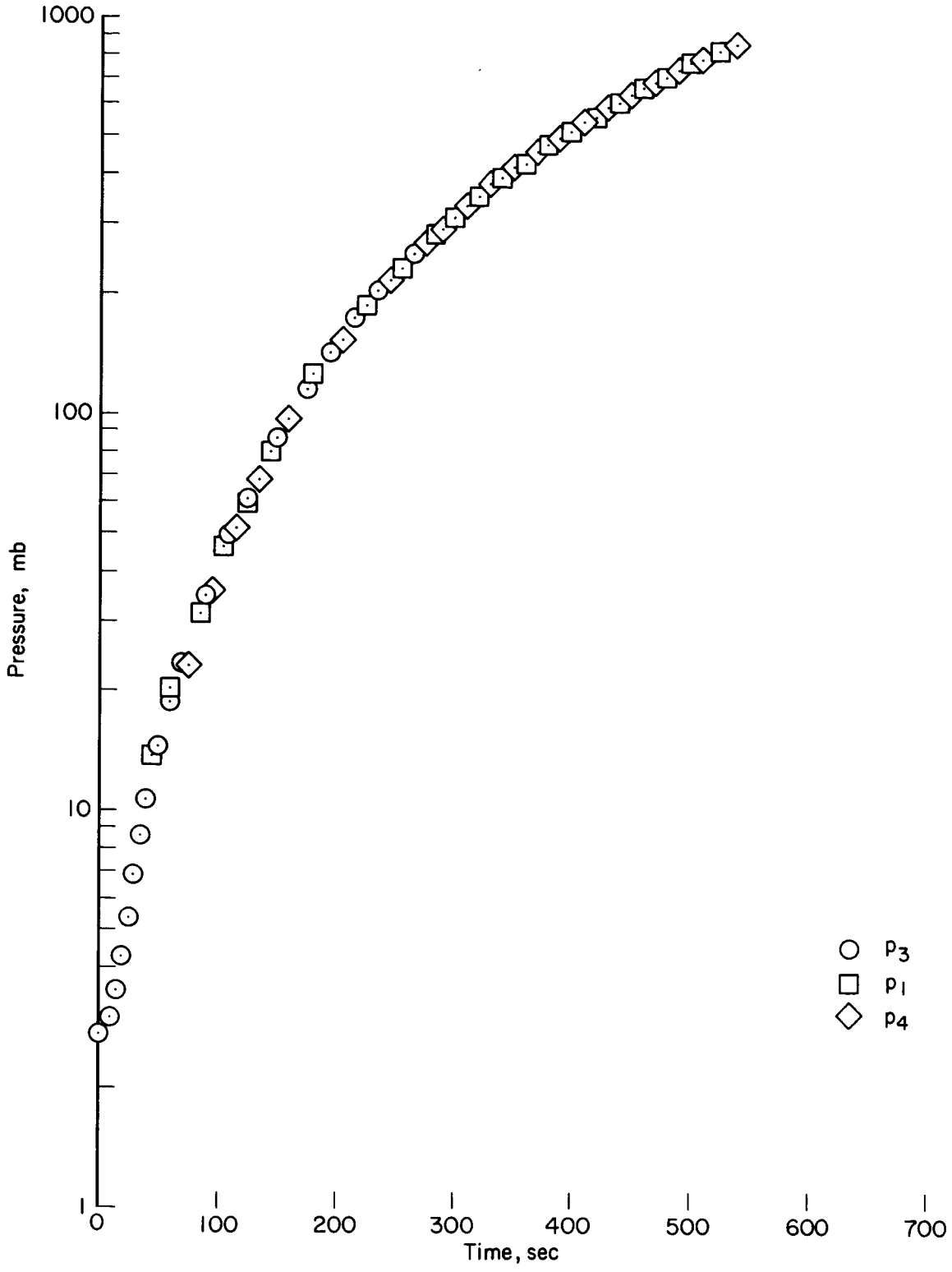

(a) Pressure.

Figure 2.- Measured quantities versus time.

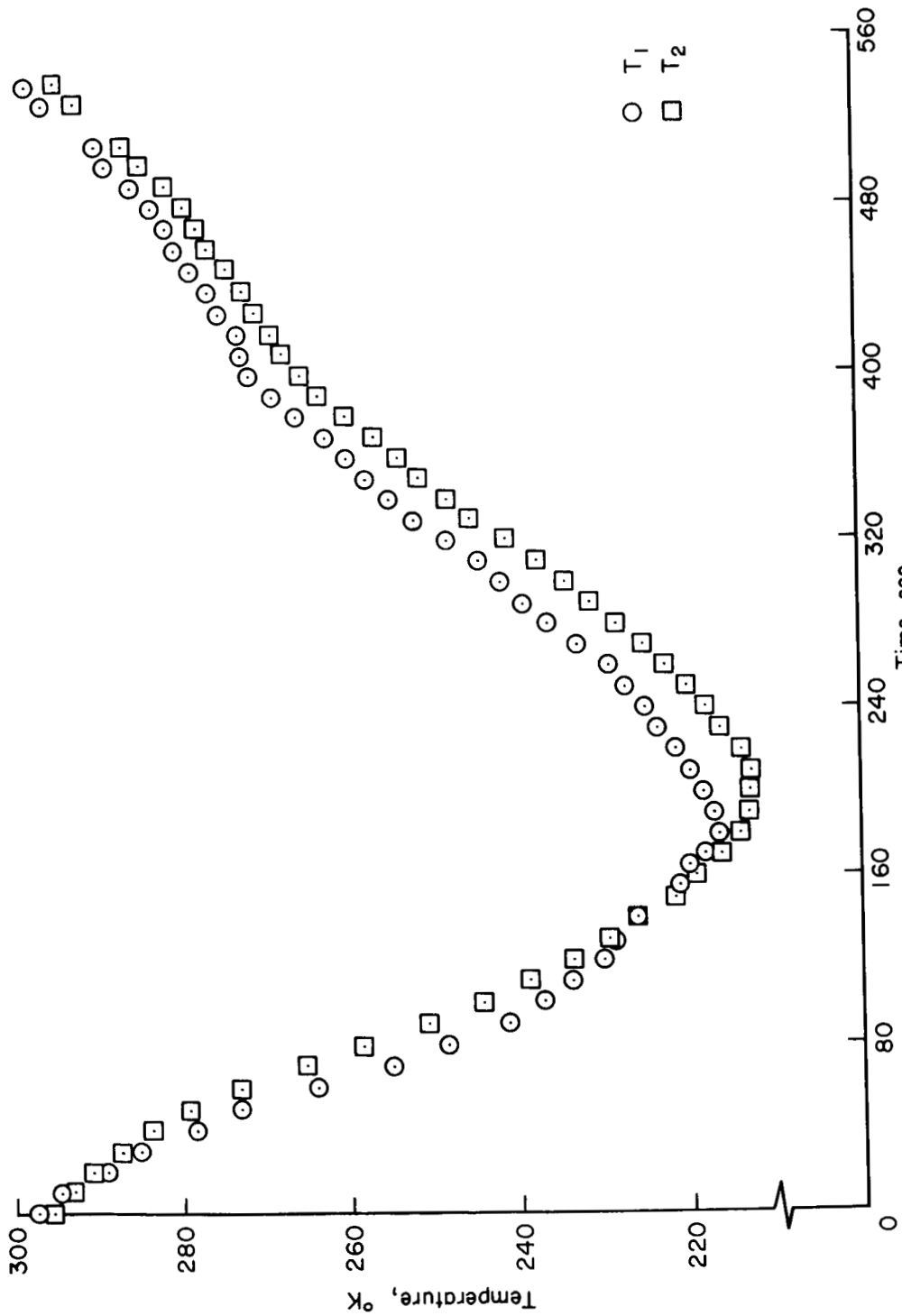

(b) Recovery temperature.

Figure 2.- Continued.

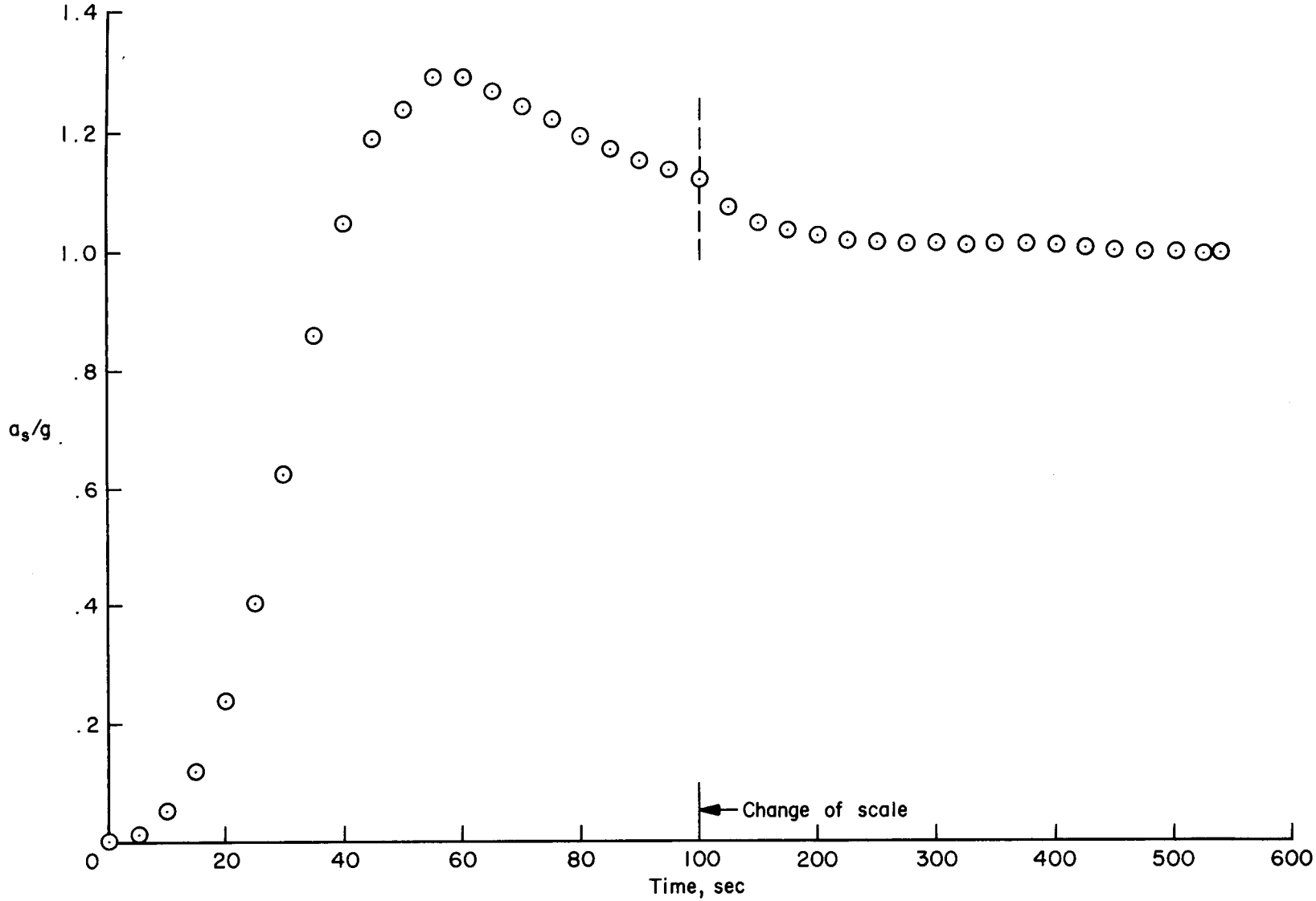

(c) Aerodynamic acceleration.

Figure 2.- Concluded.

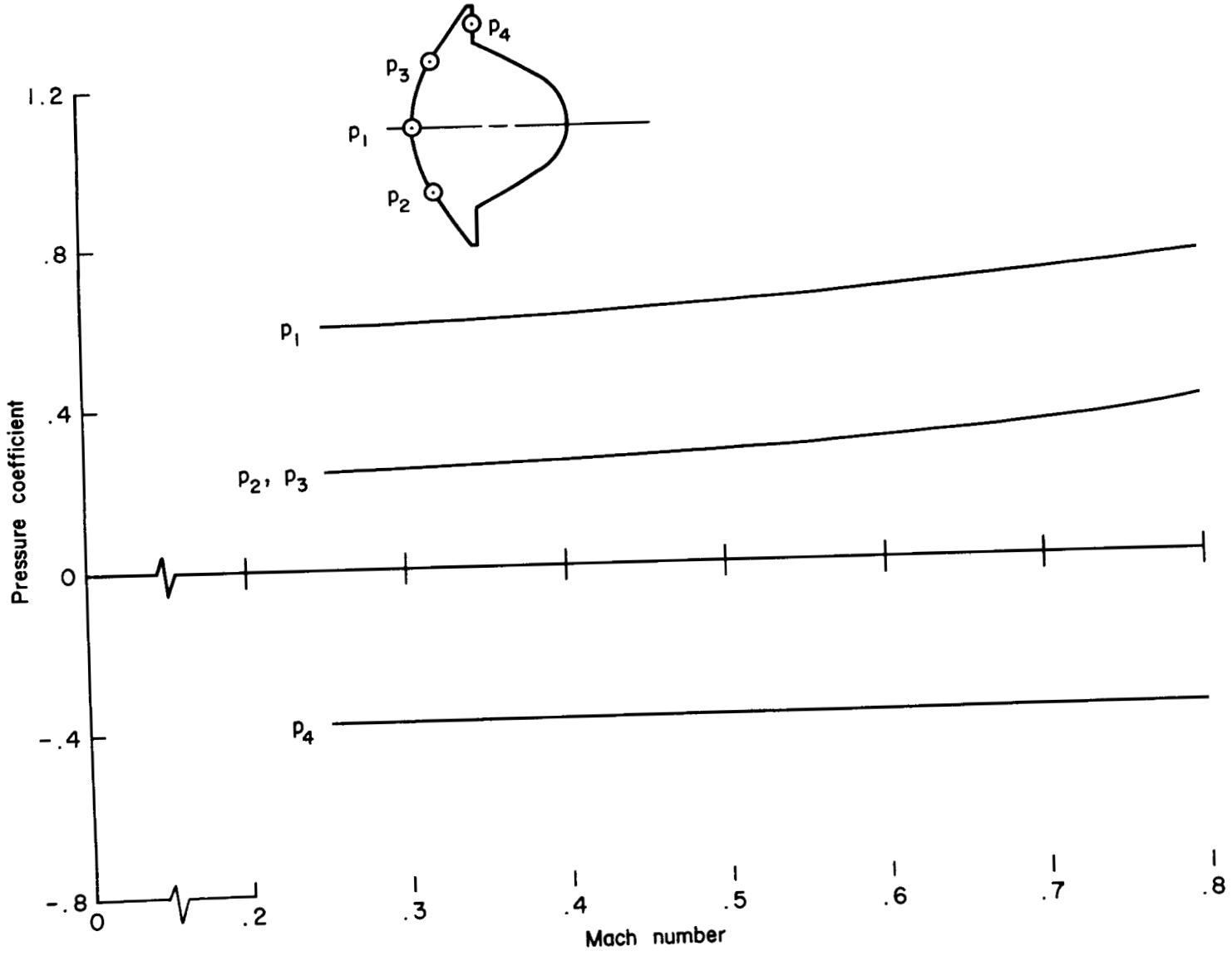

Figure 3.- Pressure coefficient versus Mach number ($\alpha = 0^{\circ}$).

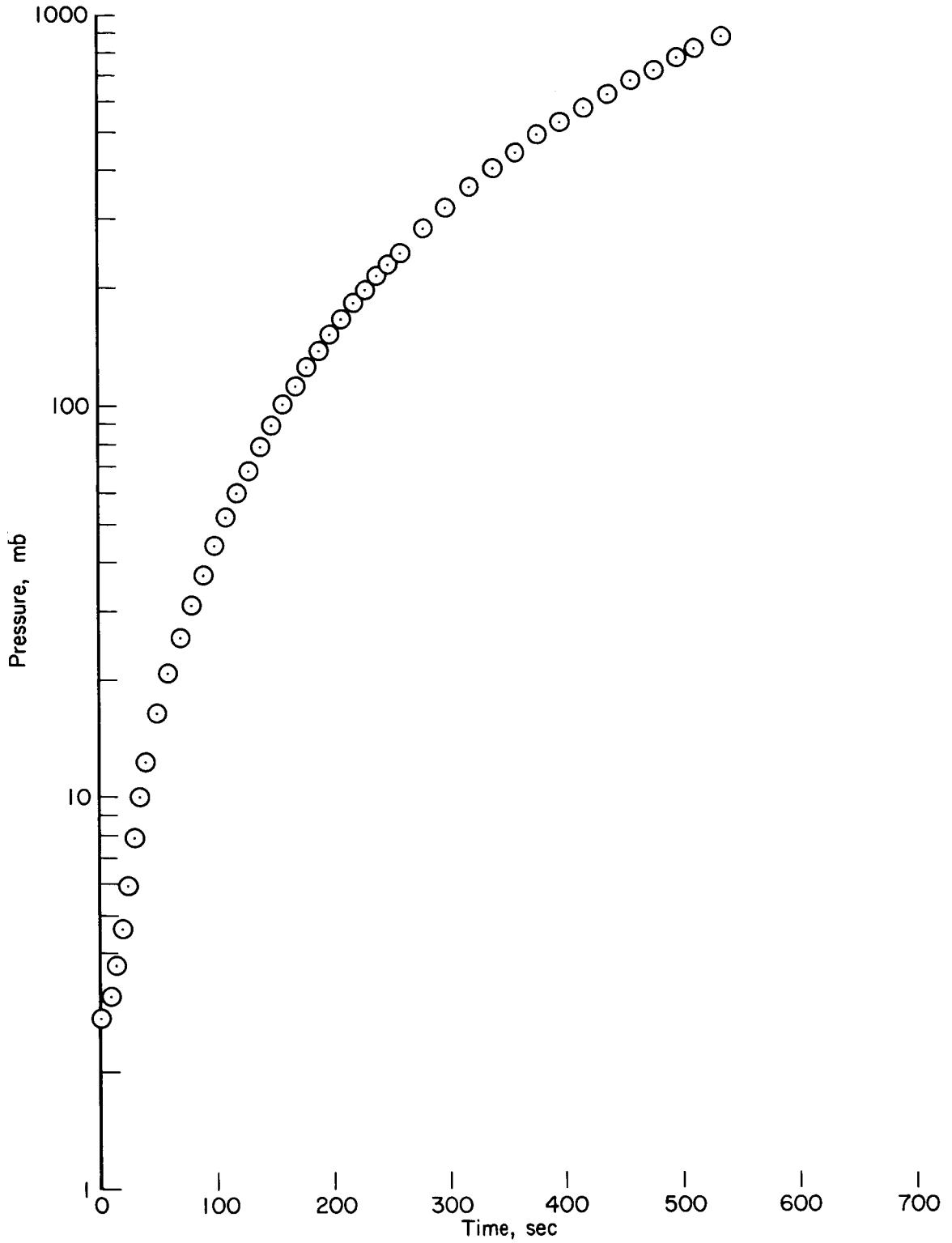

Figure 4.- Average of stagnation pressure, given by three sensors, versus time.

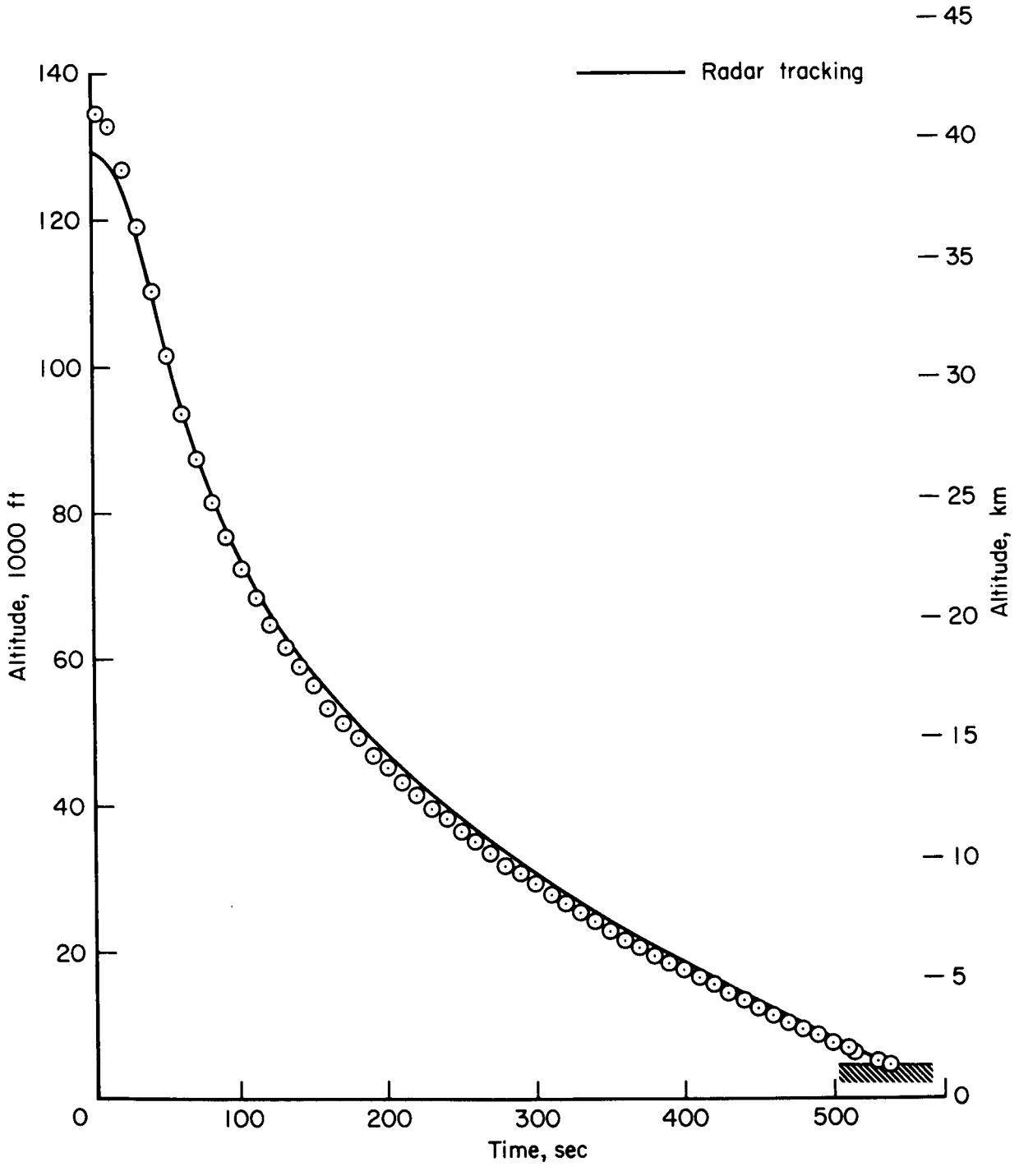

Figure 5.- Deduced altitude versus time.

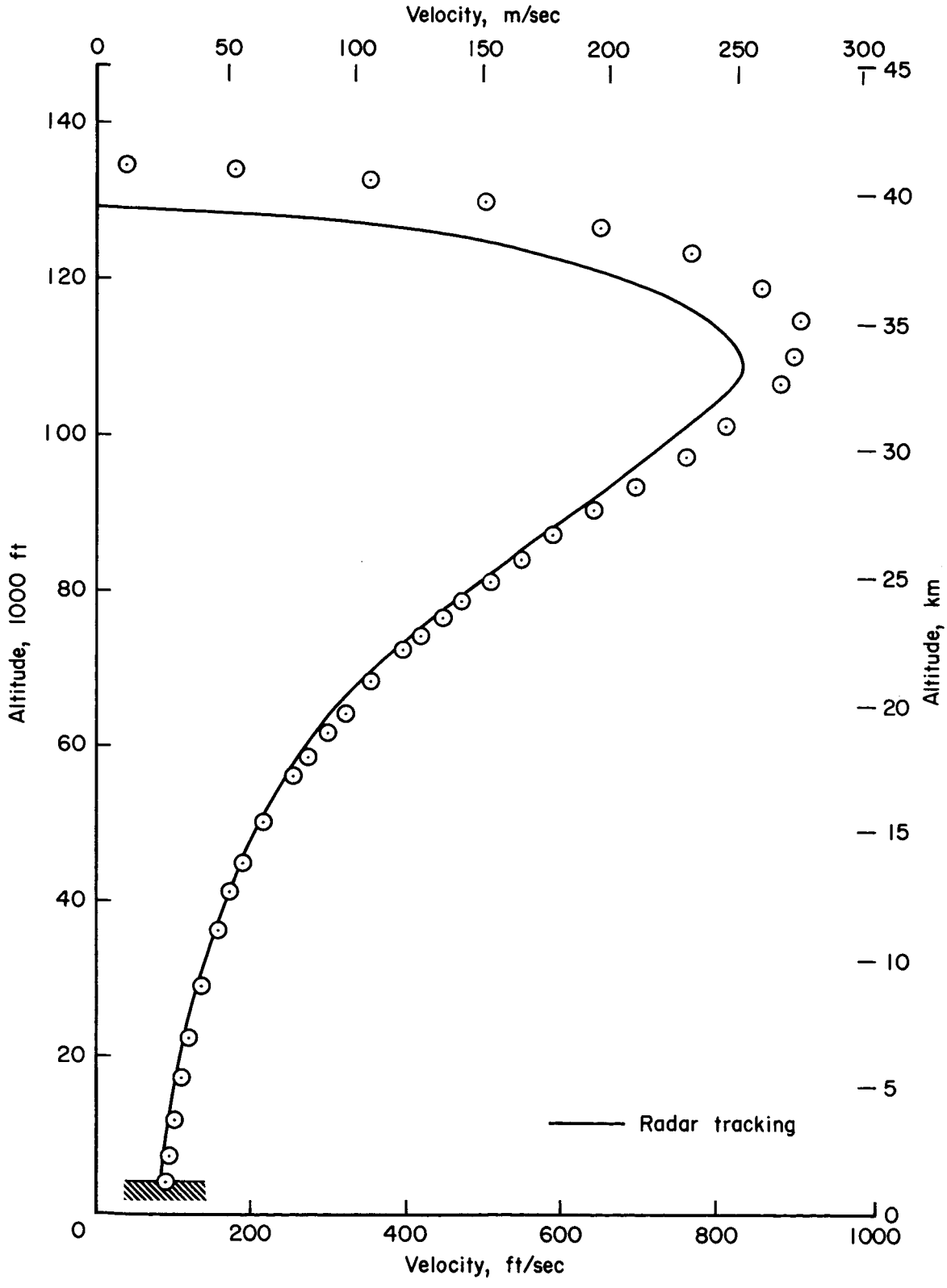

Figure 6.- Deduced altitude versus velocity.

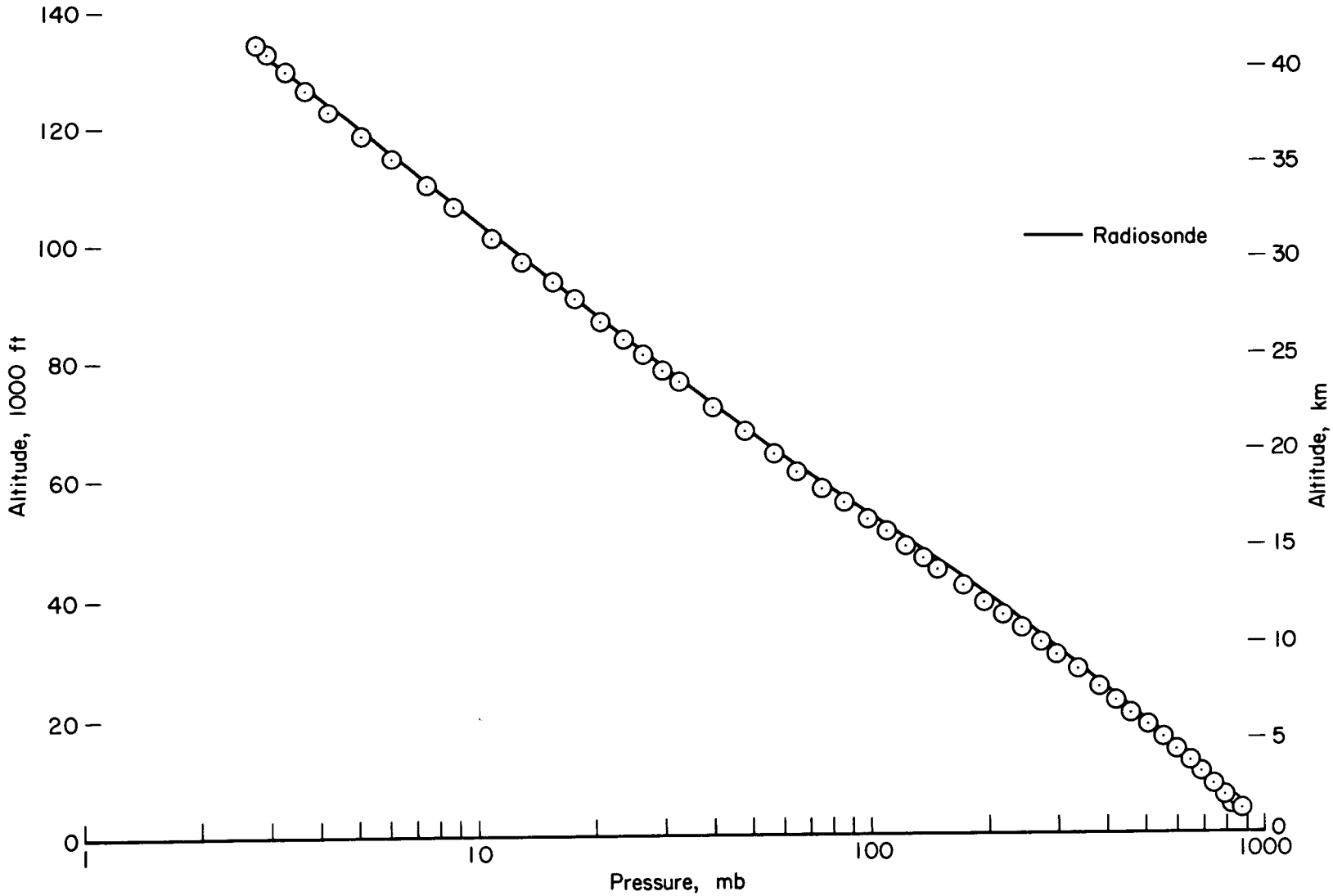

(a) Pressure.

Figure 7.- Deduced altitude versus free-stream quantities.

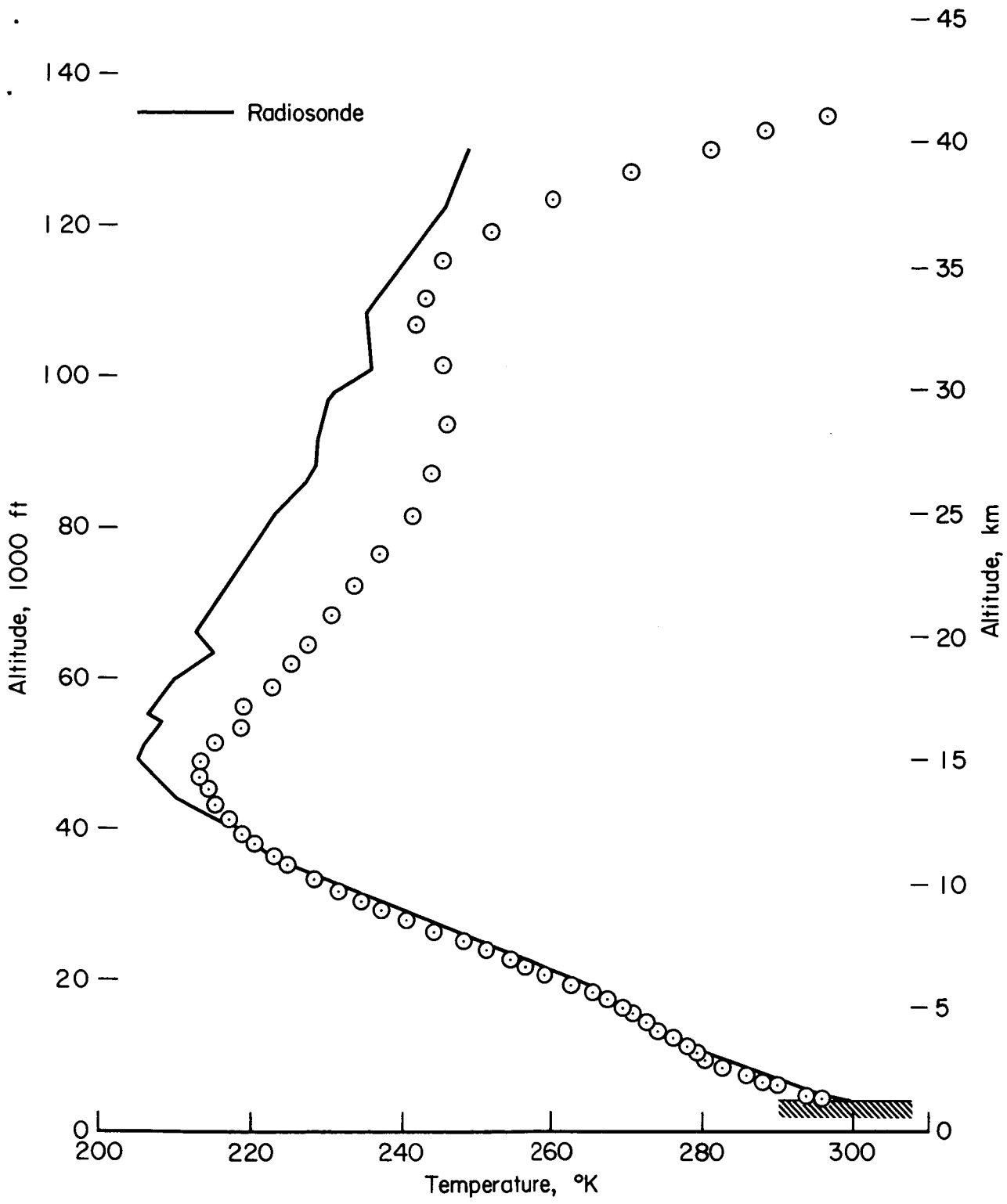

(b) Temperature.

Figure 7.- Continued.

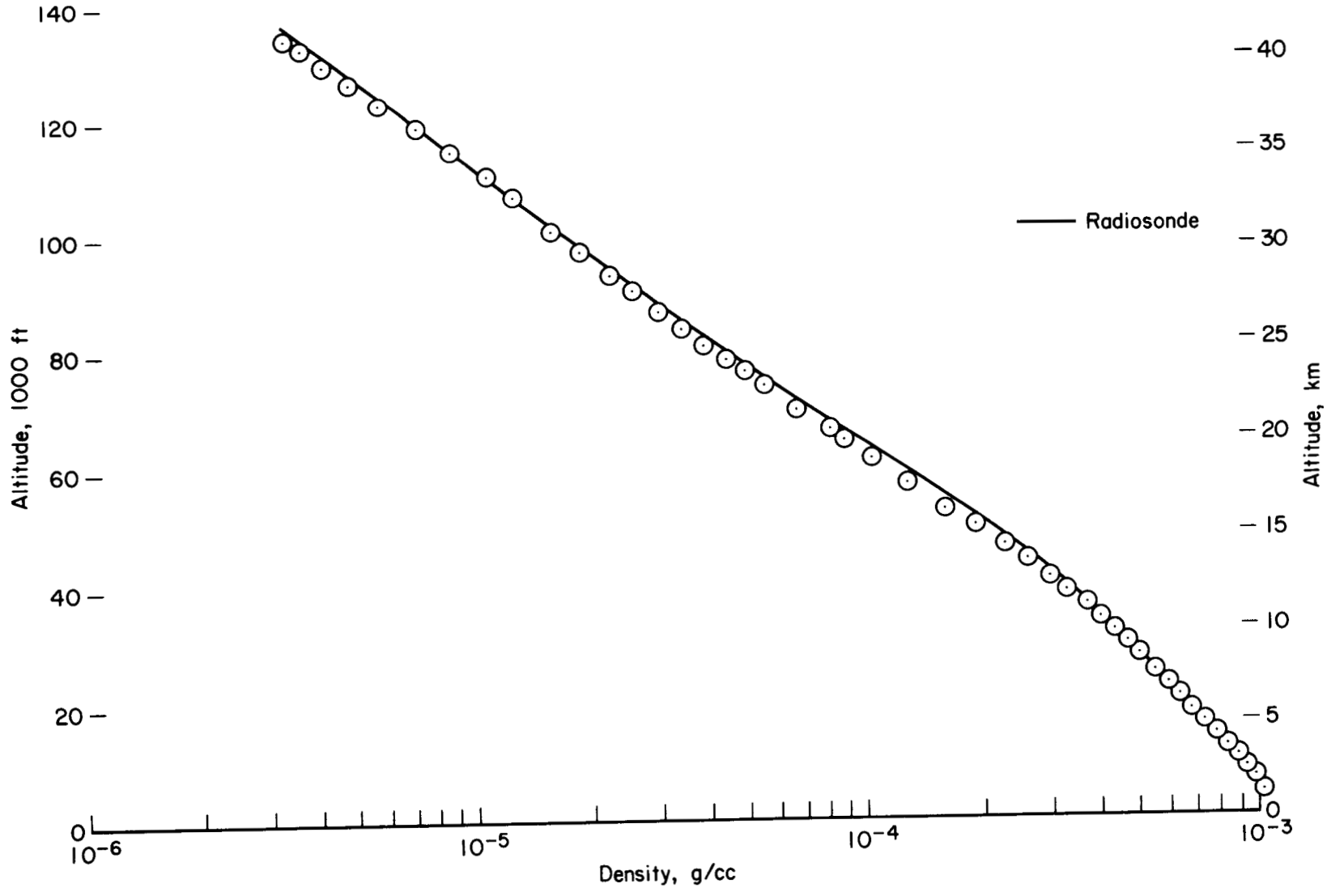

(c) Density.

Figure 7.- Concluded.

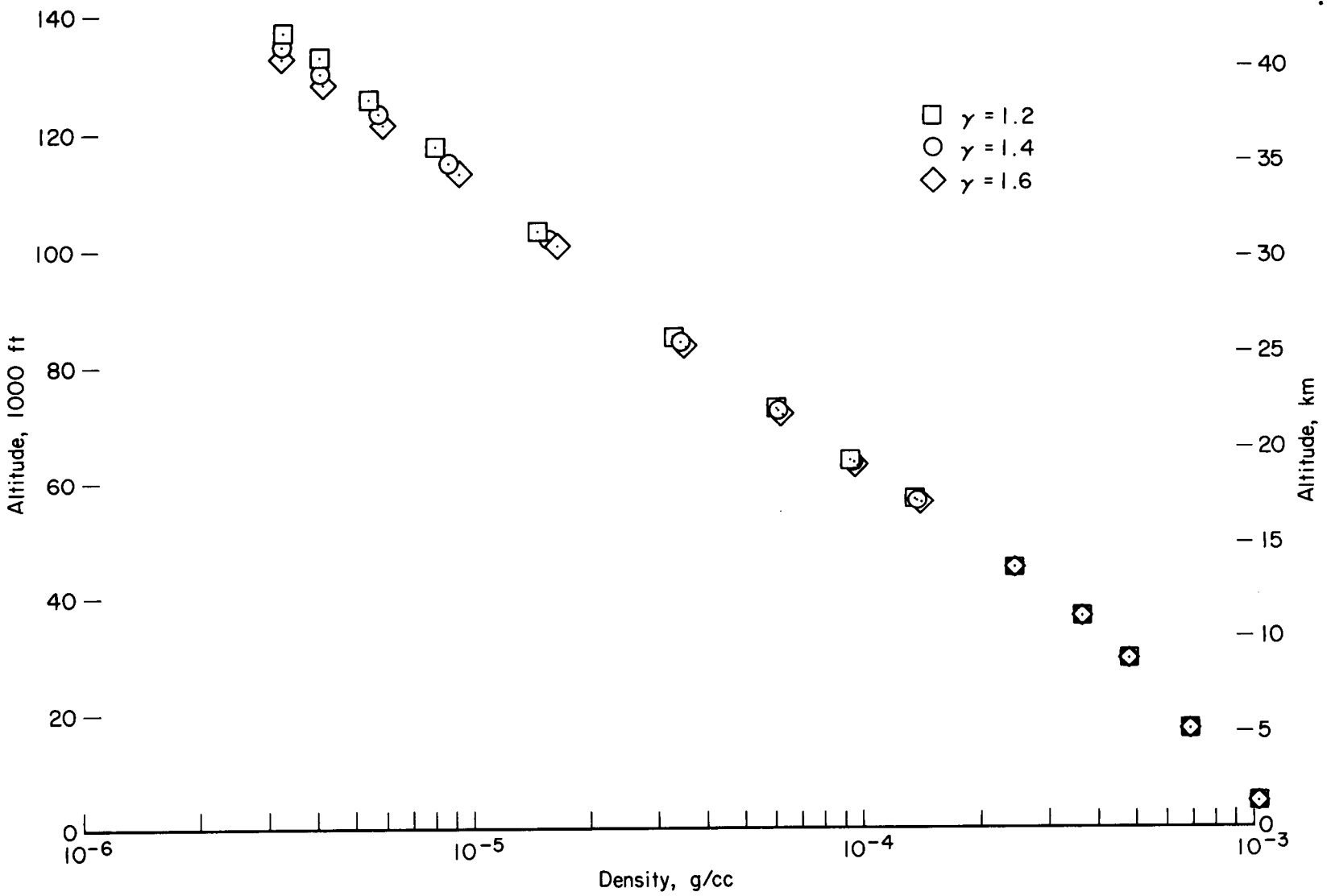

Figure 8.- Effect of γ on atmosphere structure.

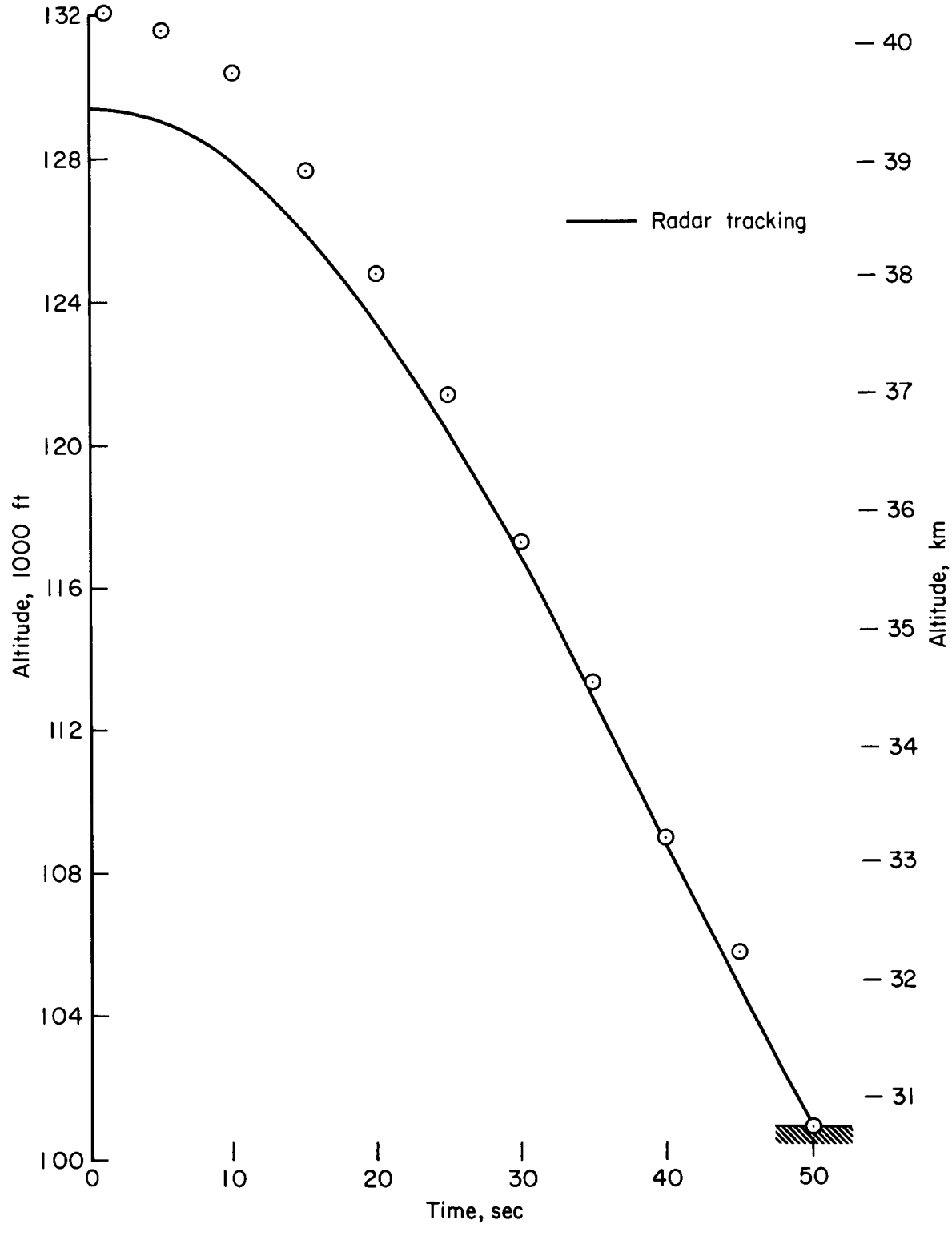

Figure 9.- Deduced altitude versus time; assumed impact at 50 seconds.

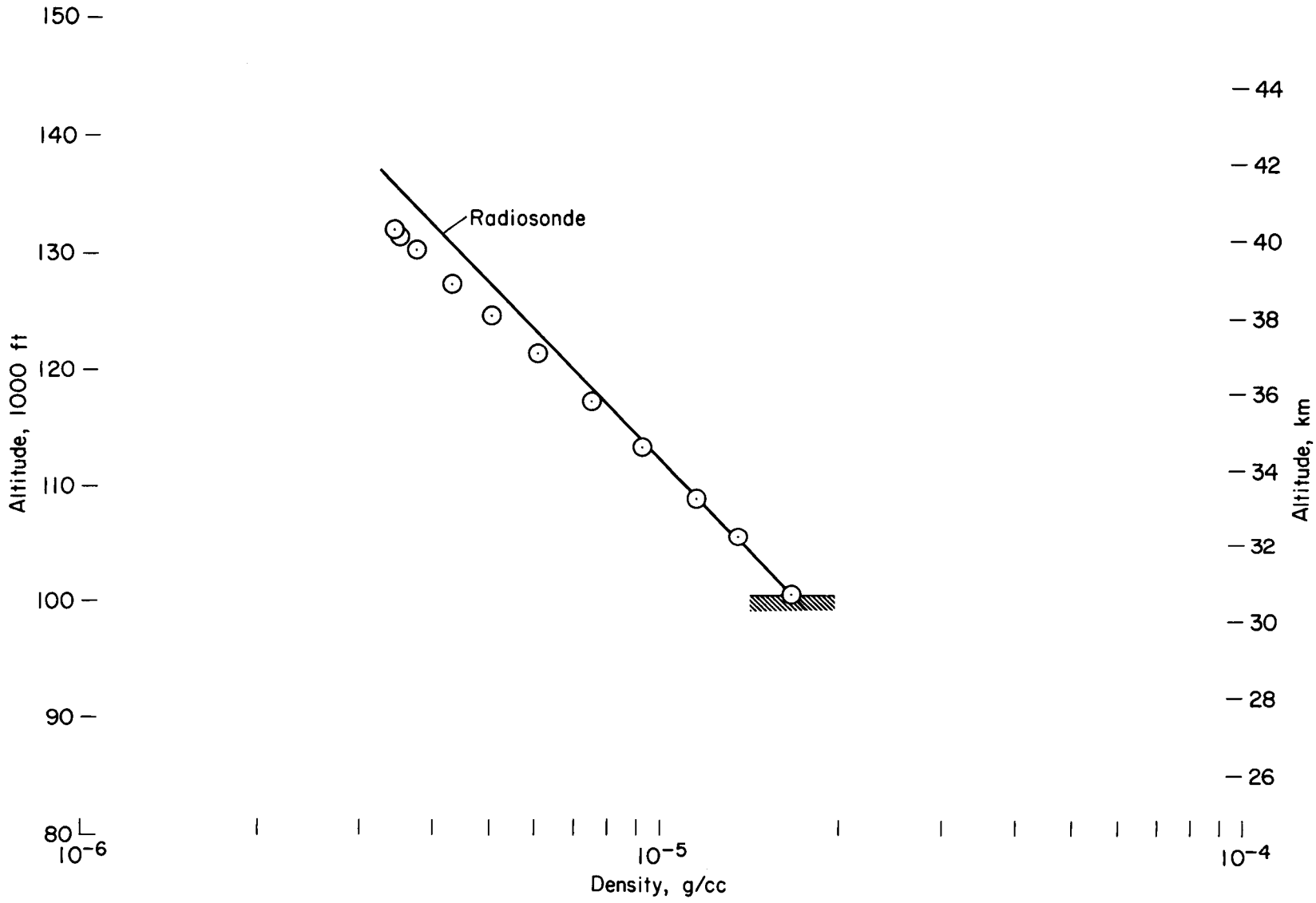

Figure 10.- Deduced altitude versus density; assumed impact at 50 seconds.

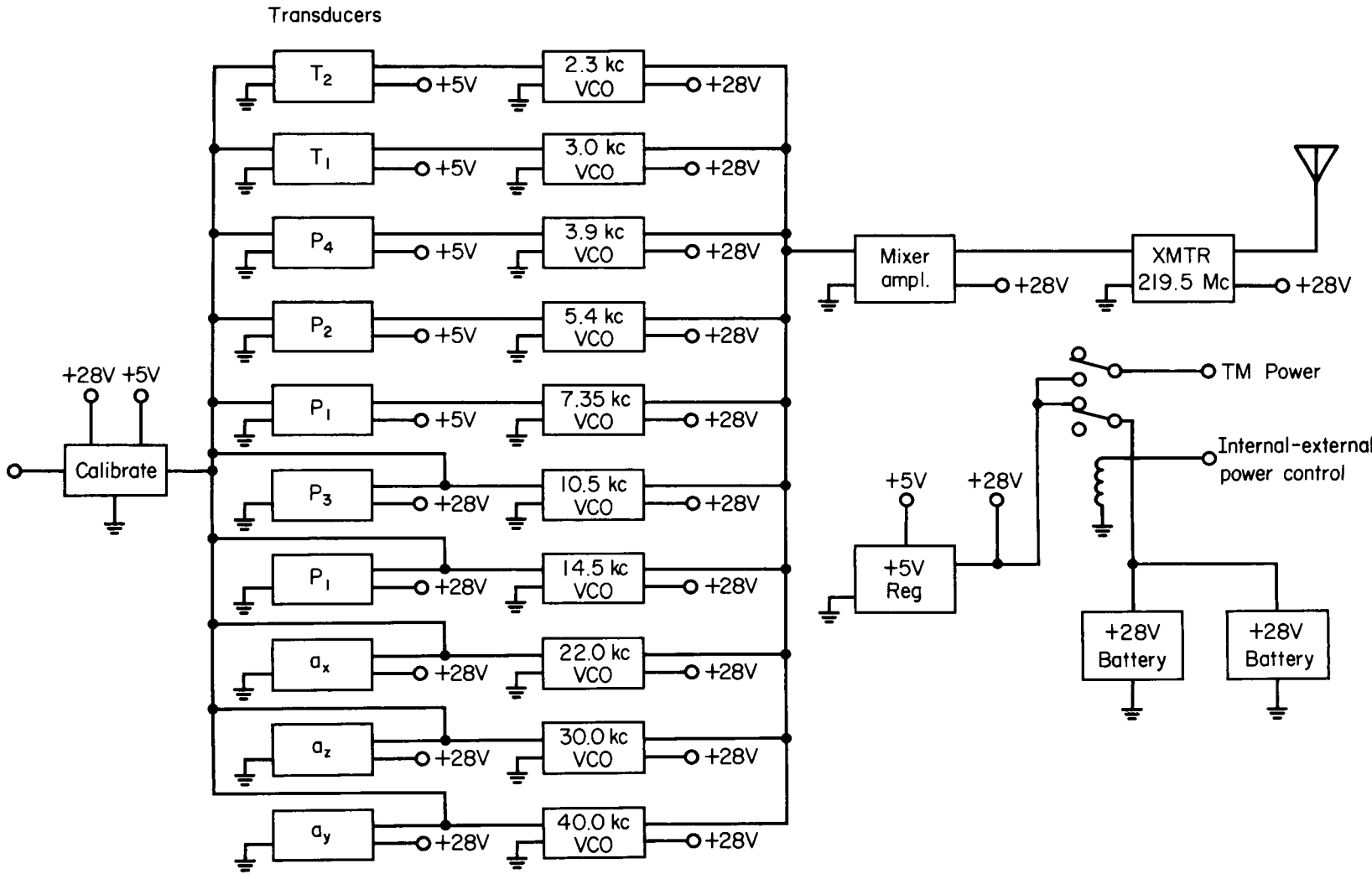

Figure 11.- Block diagram of capsule instrumentation.

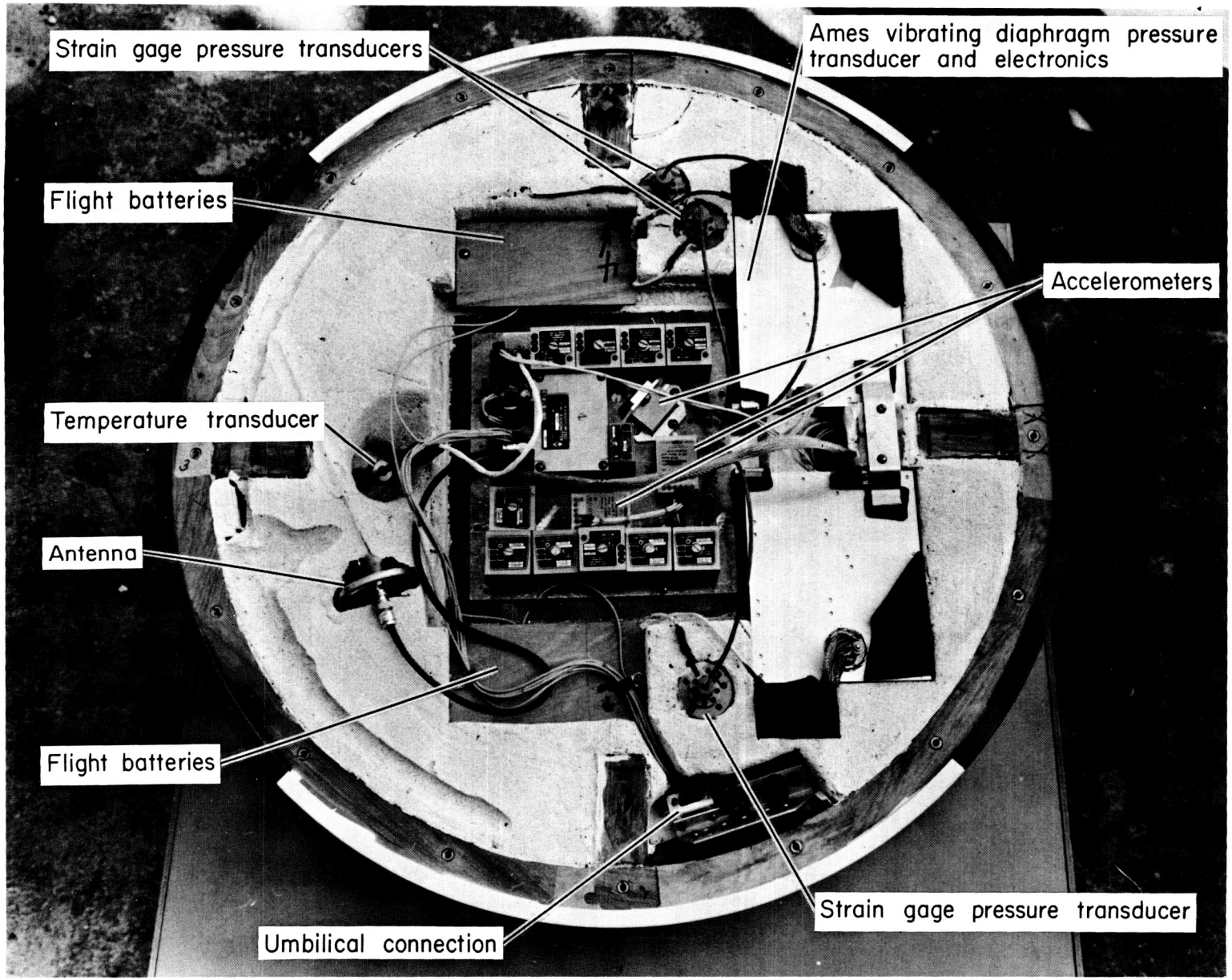

Figure 12.- Capsule instrumentation.

A-37054-3.1

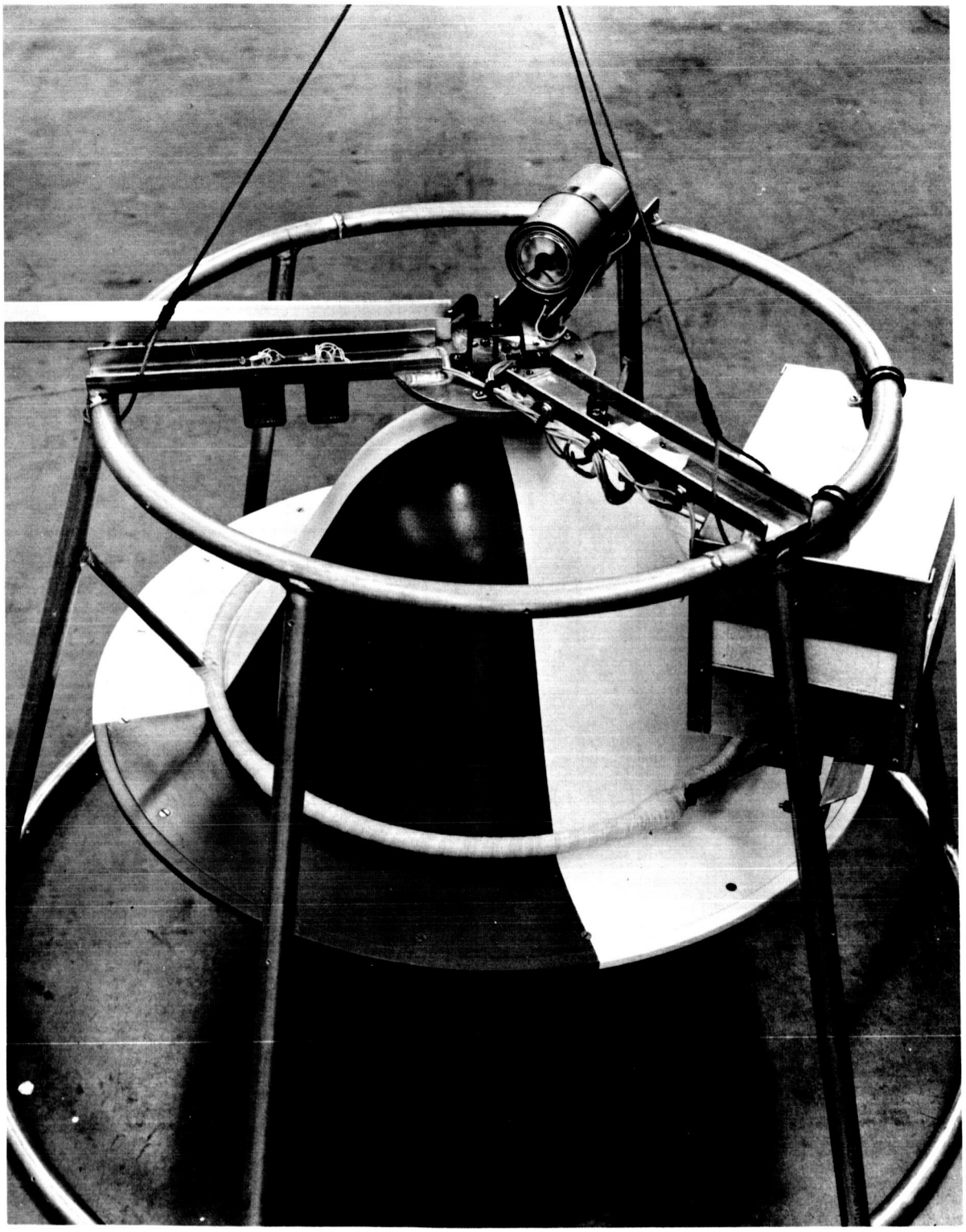

A-37054-8

Figure 13.- Hanger with capsule in place.

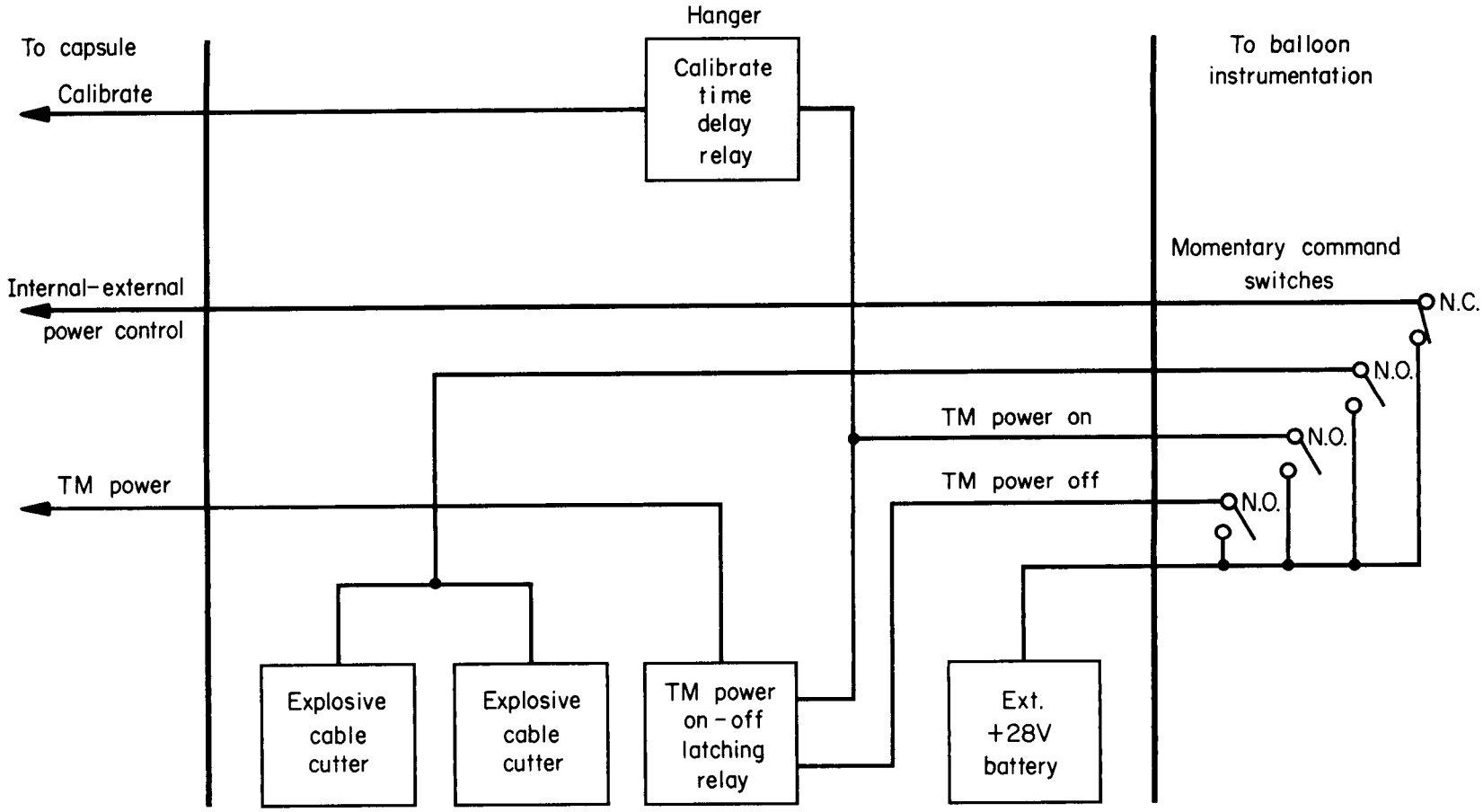

Figure 14.- Block diagram of balloon-capsule control interface.

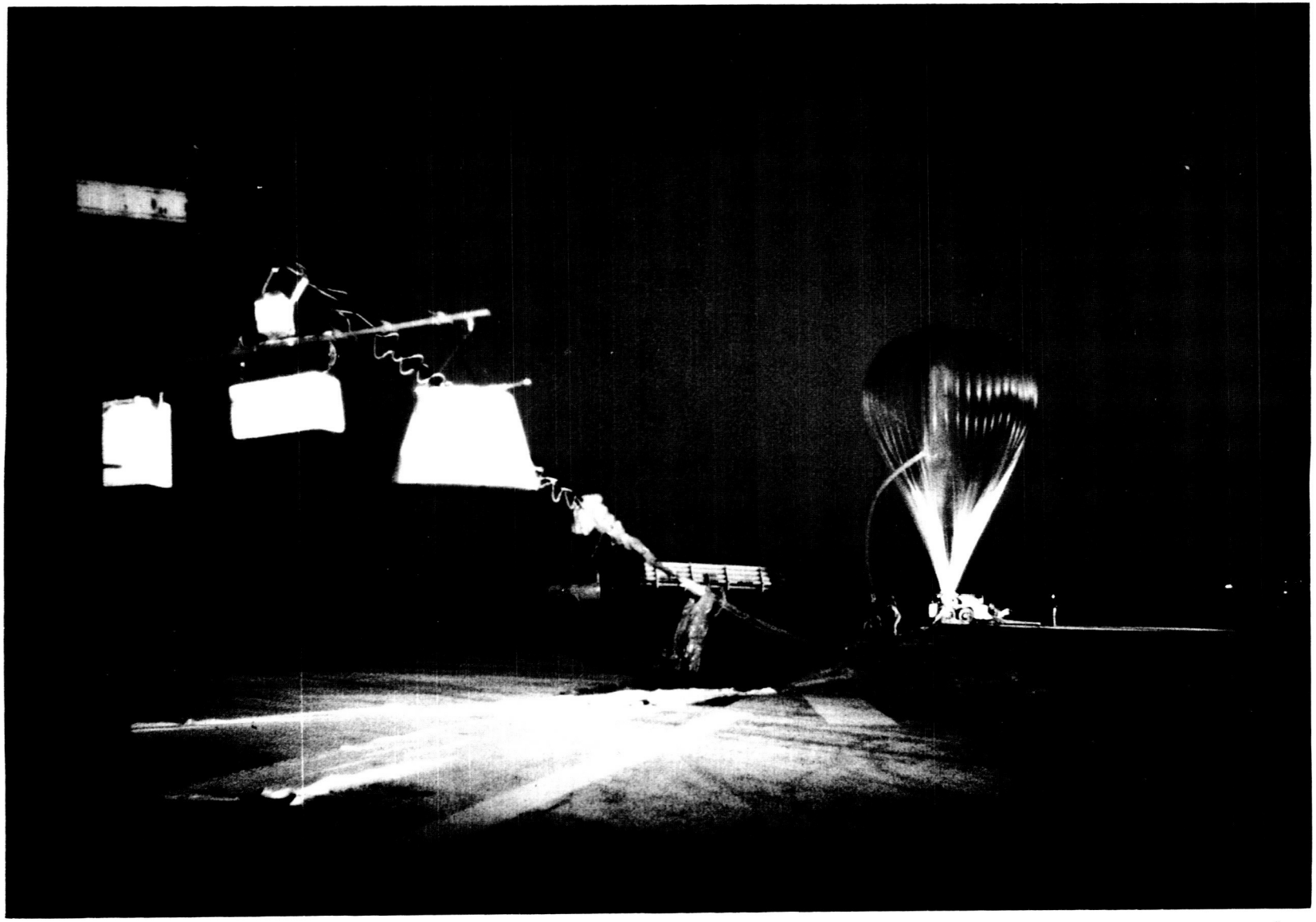

A-37326-1

(a) Before launch.

Figure 15.- Balloon-capsule system.

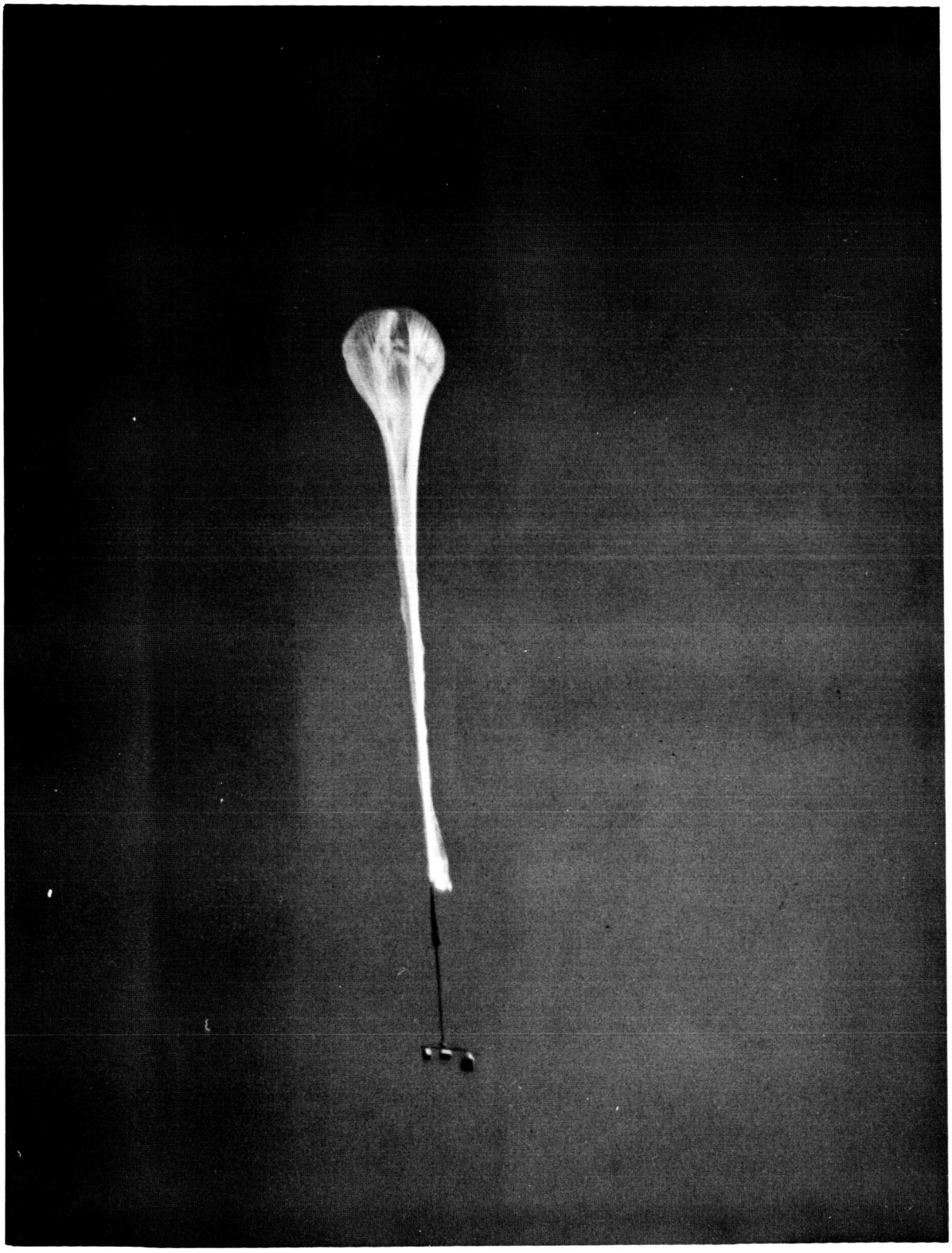

A-37326-2

(b) After launch.

Figure 15.- Concluded.

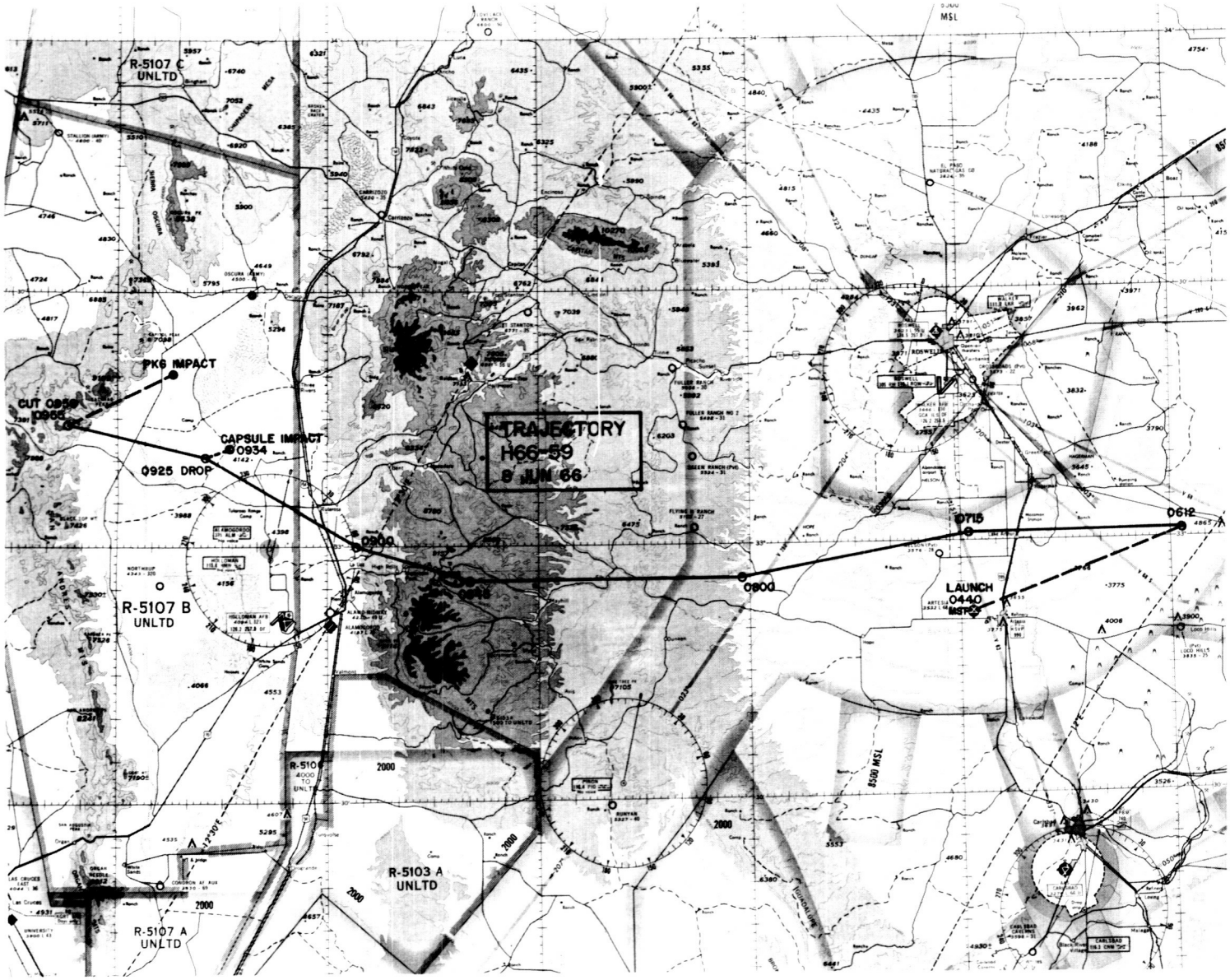

Figure 16.- Balloon trajectory.

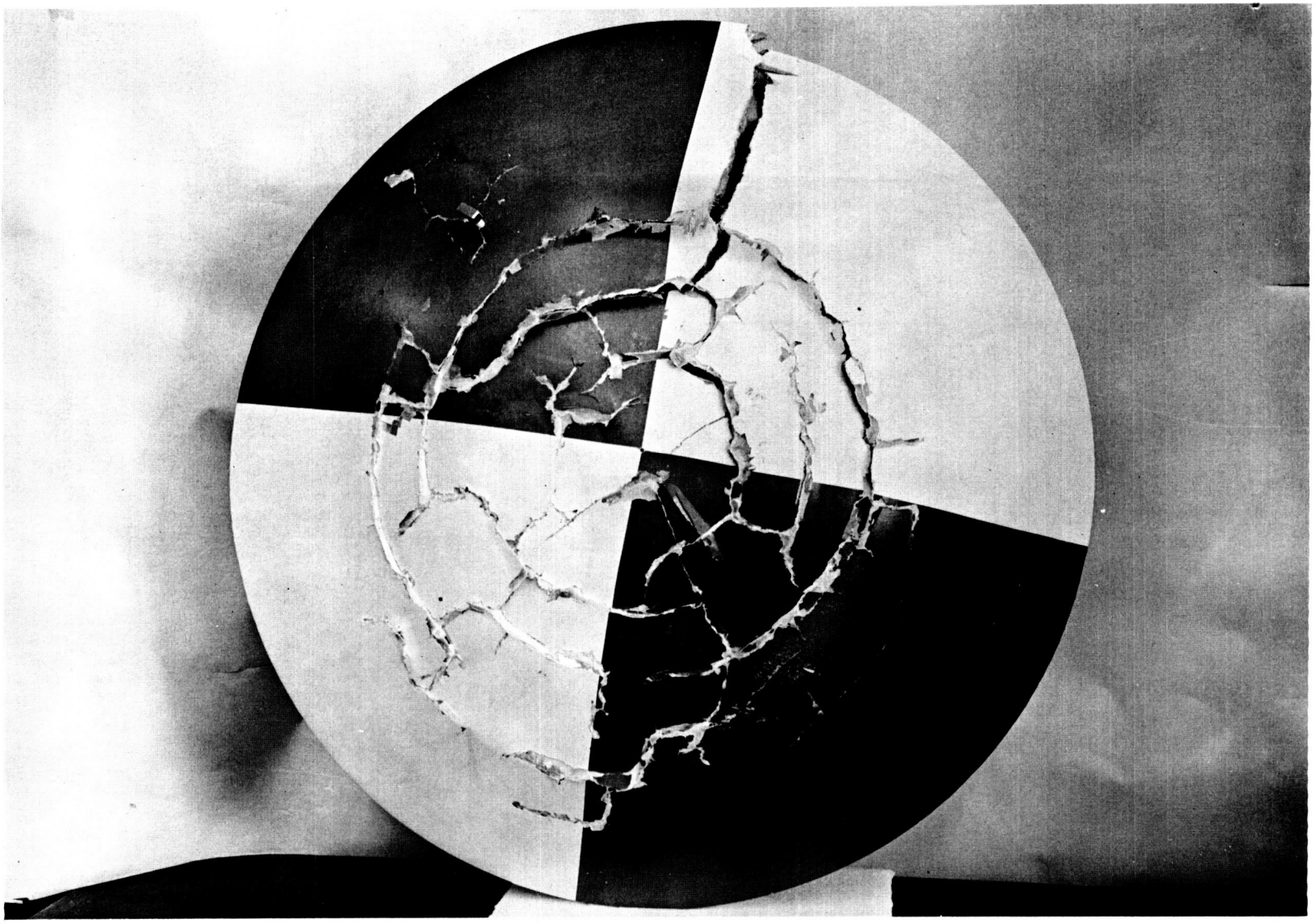

A-37326-3

Figure 17.- Recovered capsule.

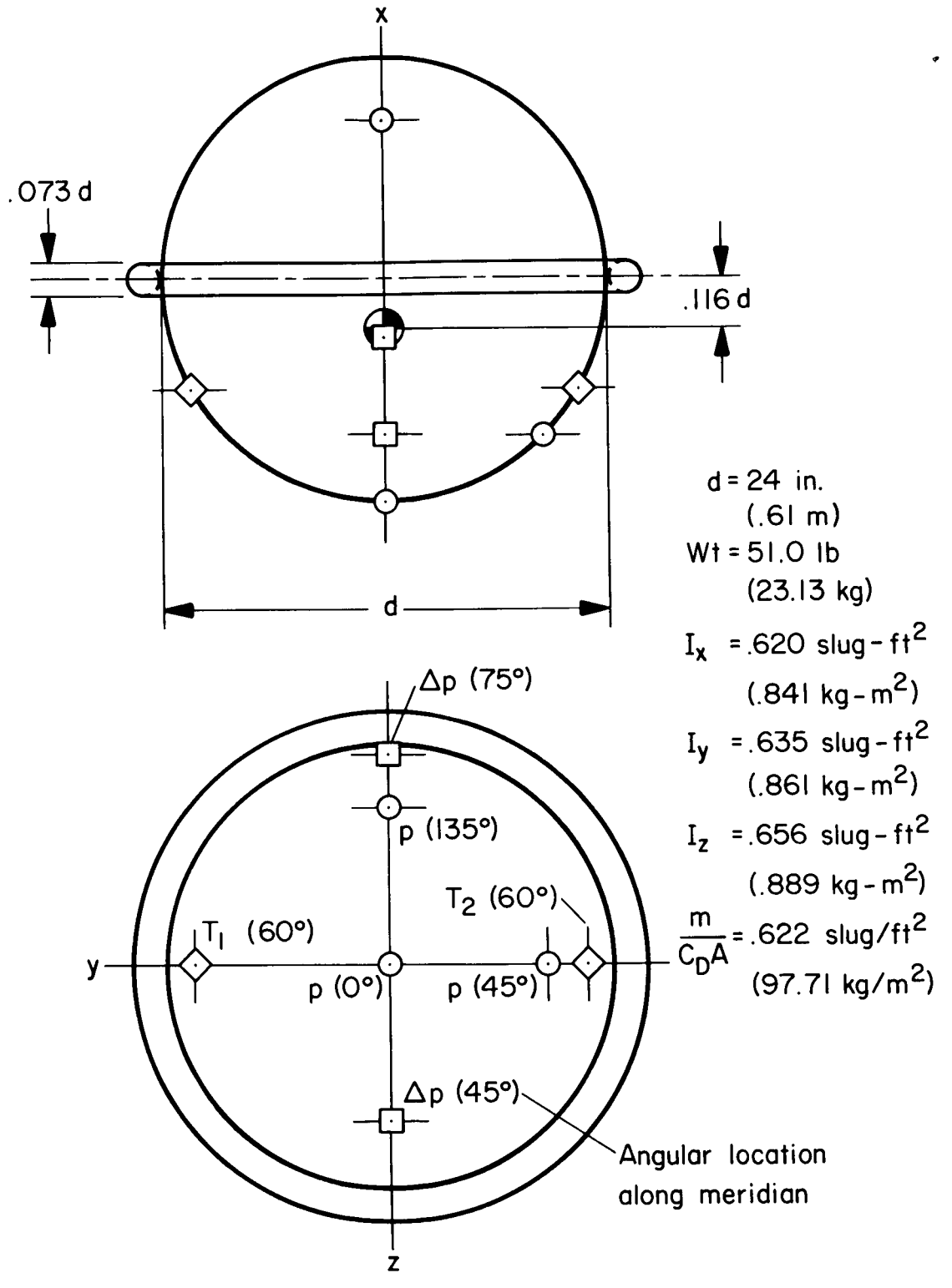

(a) Sketch and physical dimensions.

Figure 18.- Modified sphere for airplane drop.

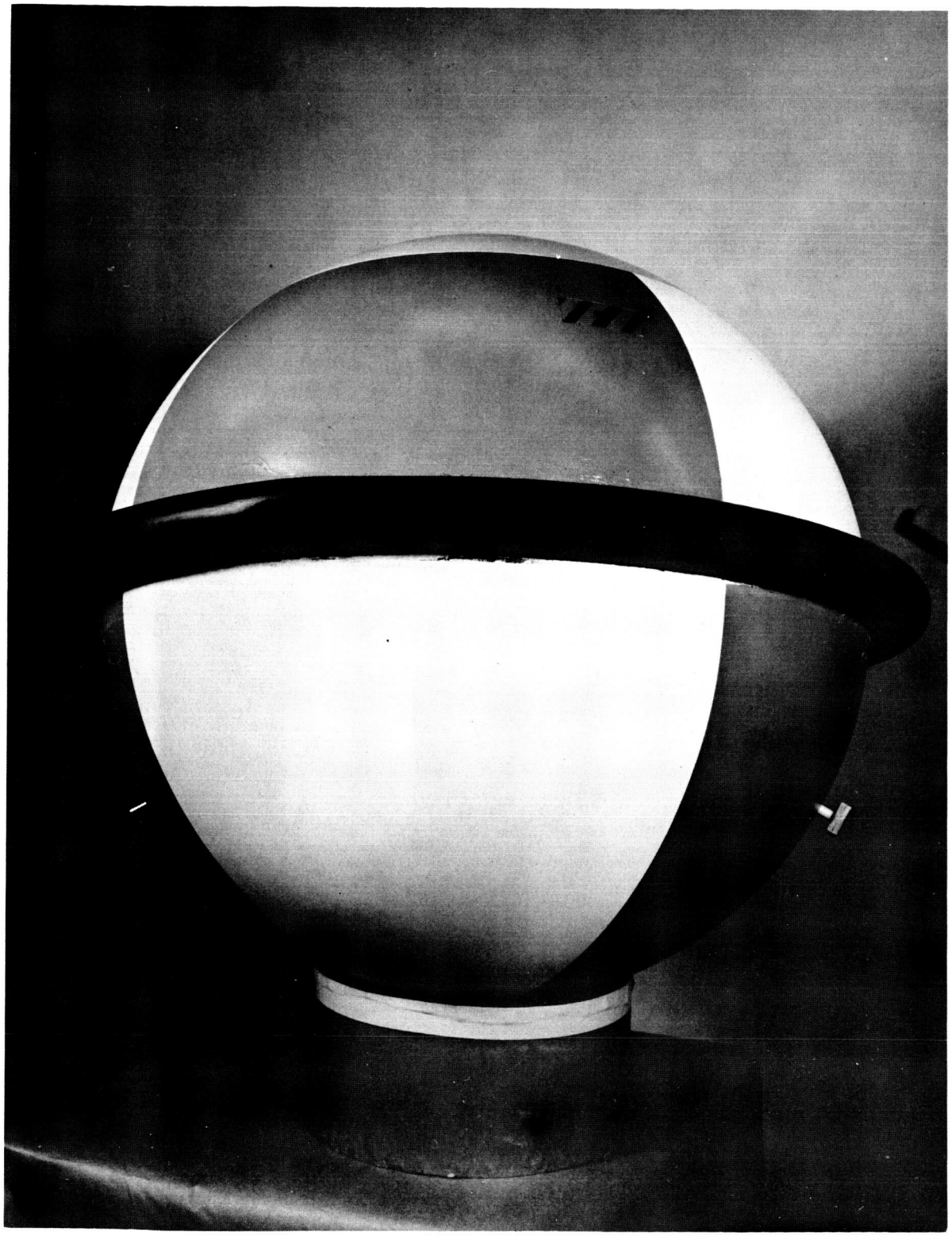

A-35290

(b) Photograph of assembled model.

Figure 18.- Concluded.

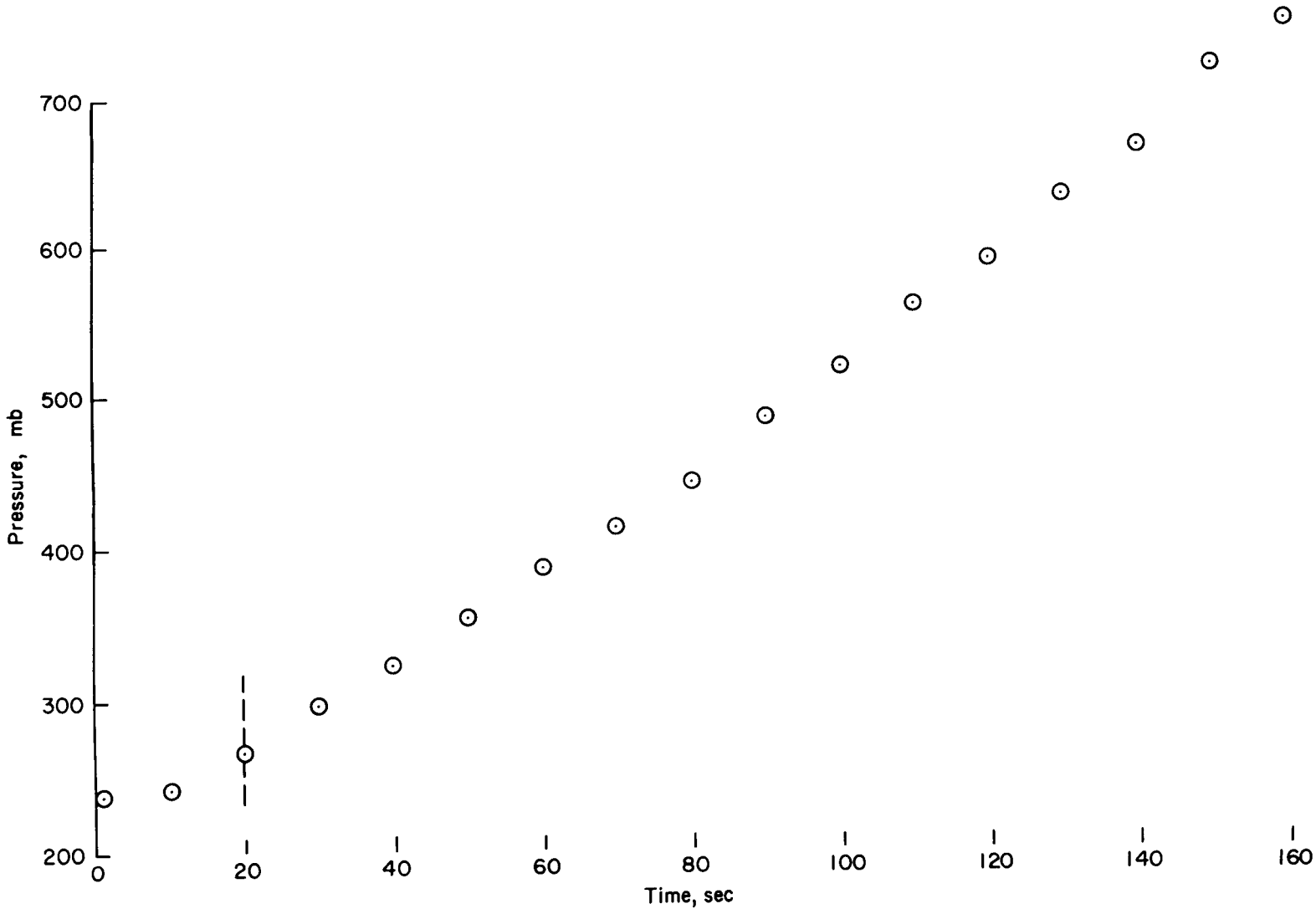

(a) Pressure.

Figure 19.- Measured quantities versus time.

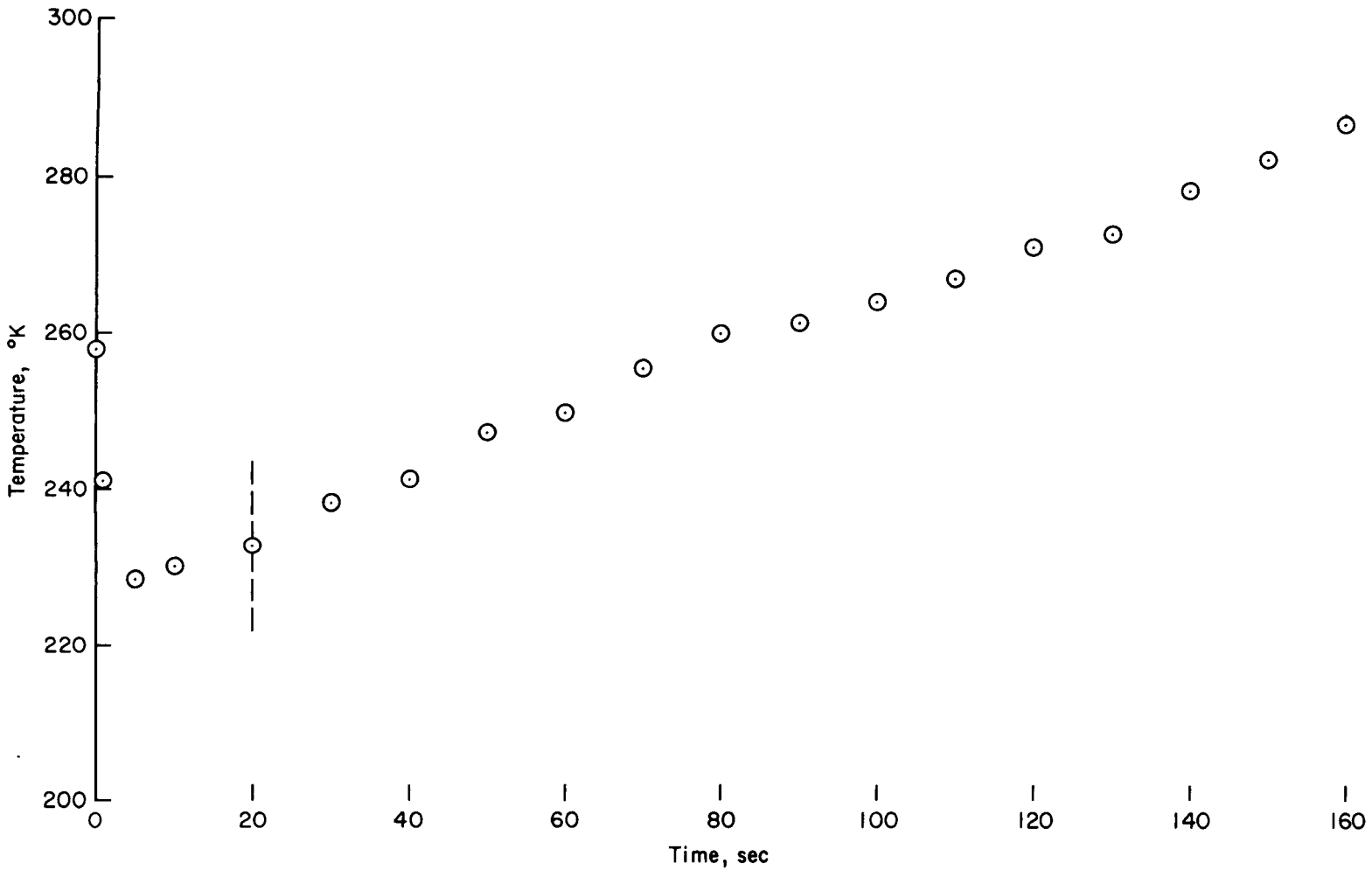

(b) Temperature.

Figure 19.- Continued.

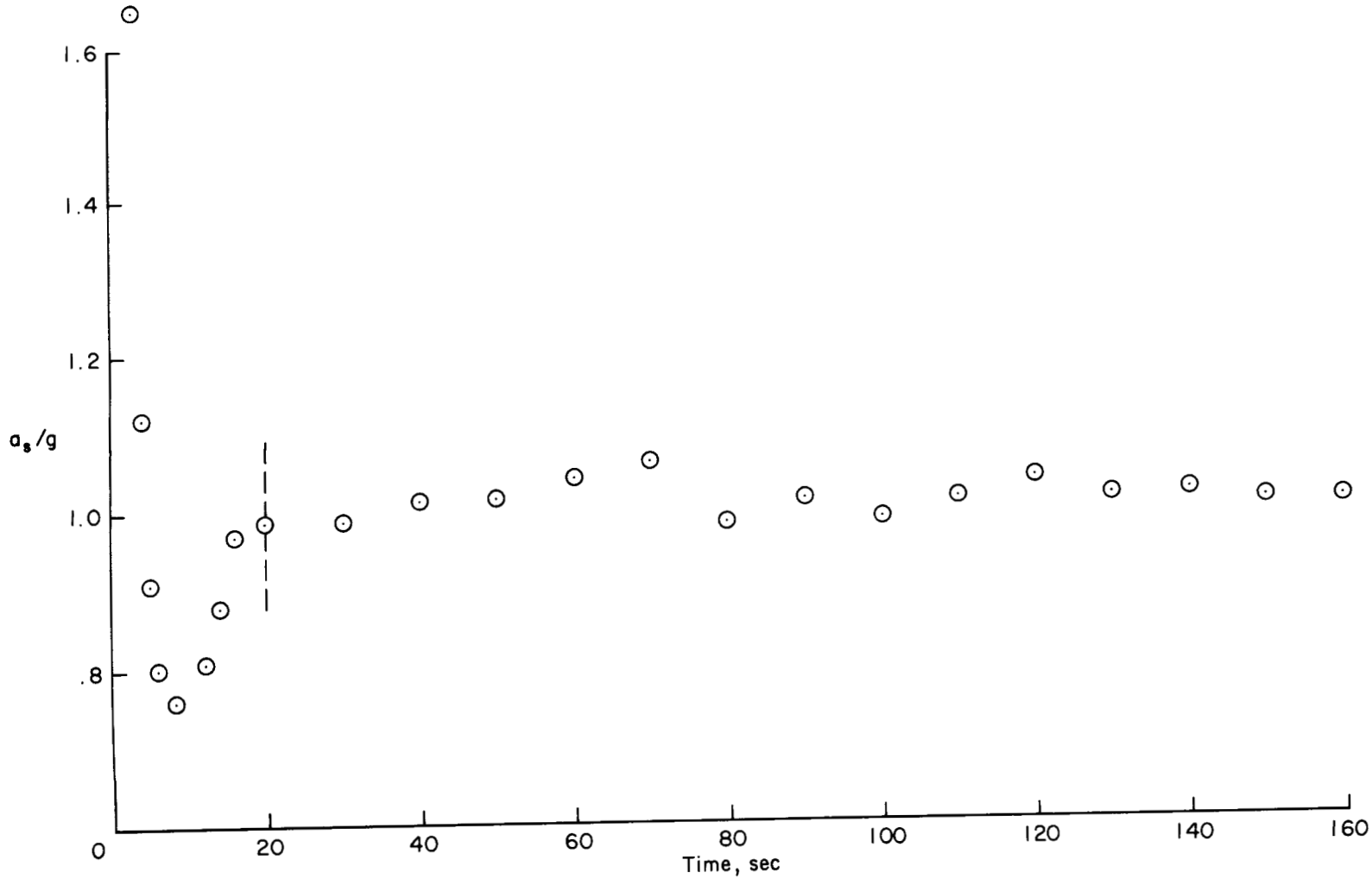

(c) Aerodynamic acceleration.

Figure 19.- Concluded.

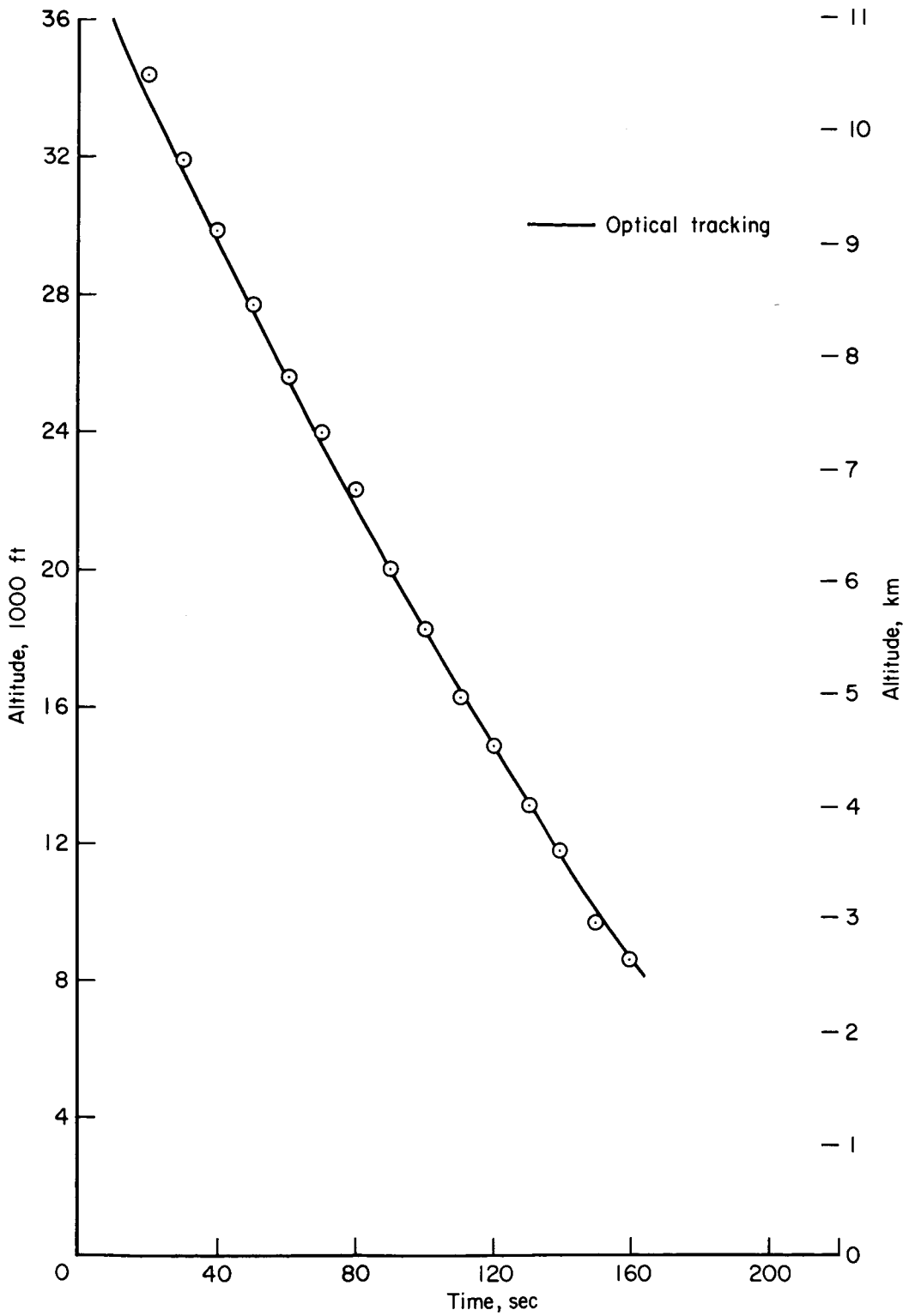

Figure 20.- Deduced altitude versus time.

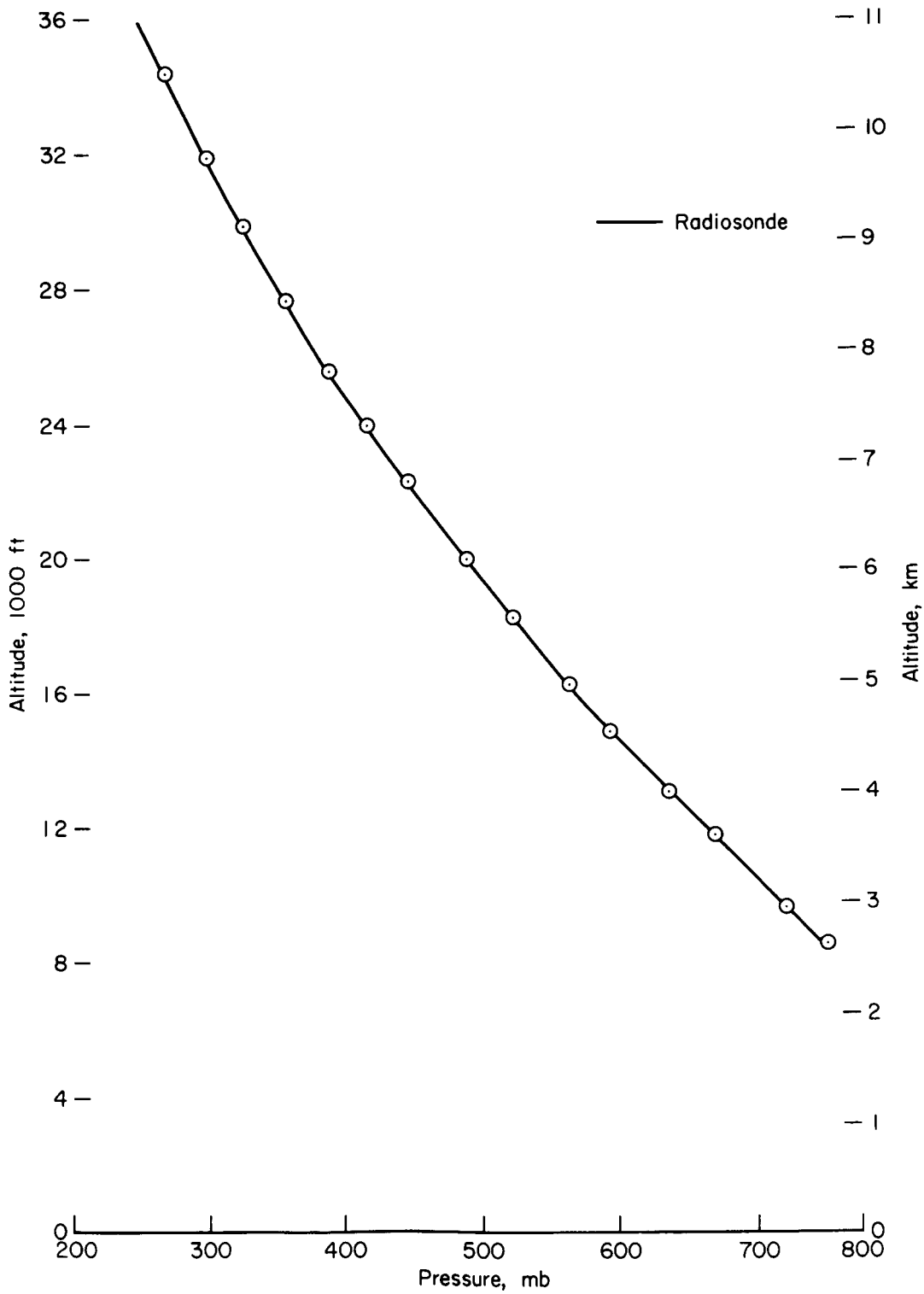

(a) Pressure

Figure 21.- Deduced altitude versus free-stream quantities.

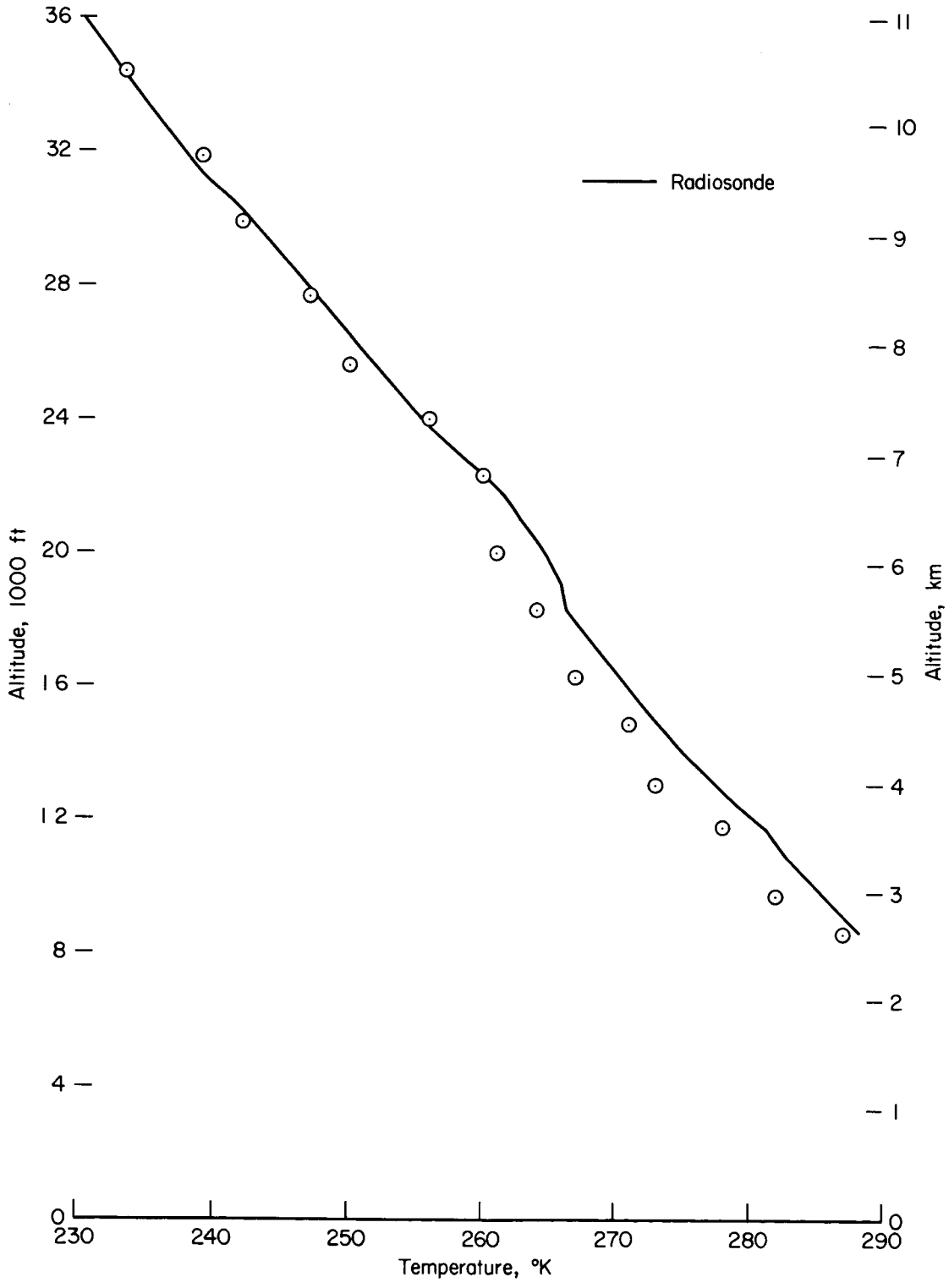

(b) Temperature.

Figure 21.- Continued.

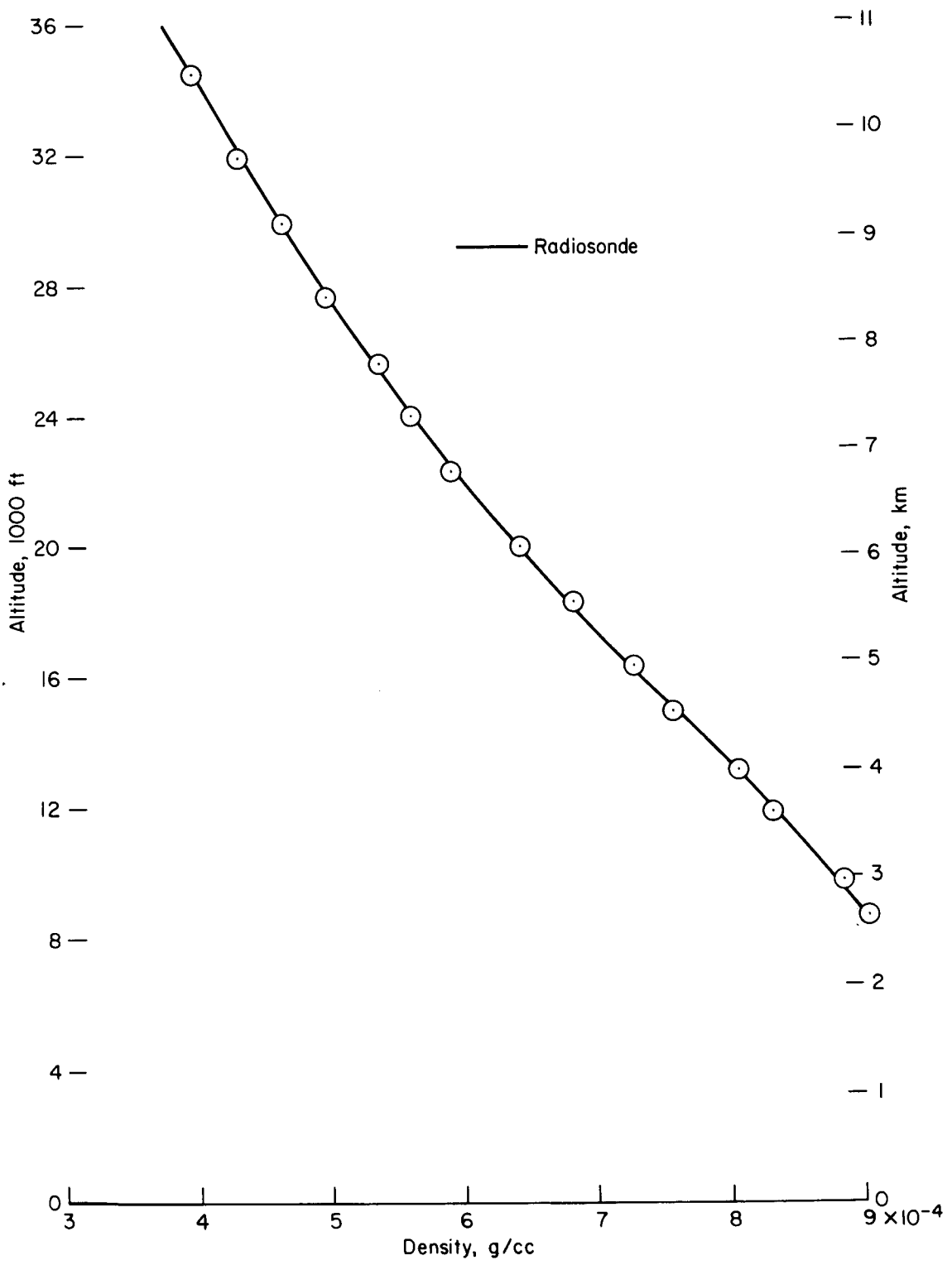

(c) Density

Figure 21.- Concluded.

NASA-Langley, 1967 — 13 A-2516

"The aeronautical and space activities of the United States shall be conducted so as to contribute . . . to the expansion of human knowledge of phenomena in the atmosphere and space. The Administration shall provide for the widest practicable and appropriate dissemination of information concerning its activities and the results thereof."

—NATIONAL AERONAUTICS AND SPACE ACT OF 1958

NASA SCIENTIFIC AND TECHNICAL PUBLICATIONS

TECHNICAL REPORTS: Scientific and technical information considered important, complete, and a lasting contribution to existing knowledge.

TECHNICAL NOTES: Information less broad in scope but nevertheless of importance as a contribution to existing knowledge.

TECHNICAL MEMORANDUMS: Information receiving limited distribution because of preliminary data, security classification, or other reasons.

CONTRACTOR REPORTS: Scientific and technical information generated under a NASA contract or grant and considered an important contribution to existing knowledge.

TECHNICAL TRANSLATIONS: Information published in a foreign language considered to merit NASA distribution in English.

SPECIAL PUBLICATIONS: Information derived from or of value to NASA activities. Publications include conference proceedings, monographs, data compilations, handbooks, sourcebooks, and special bibliographies.

TECHNOLOGY UTILIZATION PUBLICATIONS: Information on technology used by NASA that may be of particular interest in commercial and other non-aerospace applications. Publications include Tech Briefs, Technology Utilization Reports and Notes, and Technology Surveys.

Details on the availability of these publications may be obtained from:

SCIENTIFIC AND TECHNICAL INFORMATION DIVISION

NATIONAL AERONAUTICS AND SPACE ADMINISTRATION

Washington, D.C. 20546